

THE WJ-395

A 50 PERCENT EFFICIENT, 100 WATT  
S-BAND TRAVELING-WAVE TUBE

By

L. A. Roberts

15 July 1968

Contract No. 951299

This work was performed for the Jet Propulsion Laboratory,  
California Institute of Technology, sponsored by the National  
Aeronautics and Space Administration under Contract NAS7-100.

FACILITY FORM 602	N 68-36587	
	(ACCESSION NUMBER)	(THRU)
	51	
	(PAGES)	(CODE)
	CR-97222	09
	(NASA CR OR TMX OR AD NUMBER)	(CATEGORY)

Final Report

GPO PRICE \$ \_\_\_\_\_

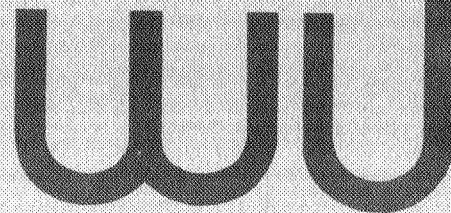
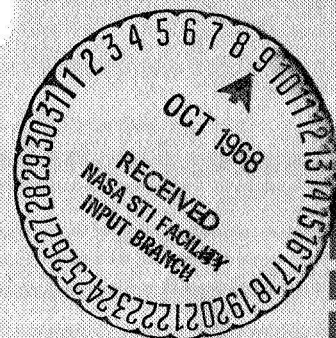
CSFTI PRICE(S) \$ \_\_\_\_\_

Hard copy (HC) \_

Microfiche (MF) \_

ff 653 July 65

Watkins-Johnson Company  
3333 Hillview Avenue  
Palo Alto, California



THE WJ-395

A 50 PERCENT EFFICIENT, 100 WATT  
S-BAND TRAVELING-WAVE TUBE

By

L. A. Roberts

15 July 1968

Contract No. 951299

This work was performed for the Jet Propulsion Laboratory,  
California Institute of Technology, sponsored by the National  
Aeronautics and Space Administration under Contract NAS7-100.

Final Report

Watkins-Johnson Company  
3333 Hillview Avenue  
Palo Alto, California

## ABSTRACT

This is the final report on a program to develop a 100 watt, 55 percent efficient traveling-wave tube at 2.295 GHz for space communication and telemetry applications.

The report describes the design basis and the operating characteristics of the final version of the tube, which is known as the WJ-395. The best overall efficiency performance (including heater) achieved was 50.5 percent at a power output level of 105 watts and a saturation gain of 38 dB. The final encapsulated version of the tube exhibits an overall efficiency greater than 49 percent. The tube is capable of meeting the shock, vibration and acceleration associated with space-craft launching and is capable of operating under space vacuum conditions using only conduction cooling.

The report also describes the state-of-the-art in high efficiency traveling-wave tubes at the inception of the program and describes developments which took place during the course of the program which had direct bearing upon its high efficiency design.





PRECEDING PAGE BLANK NOT FILMED.

## TABLE OF CONTENTS

	<u>Page No.</u>
I. PURPOSE OF THE DEVELOPMENT PROGRAM	1
II. GOALS AND ACHIEVEMENTS	1
A. Goals Established for this Development	1
B. Performance Achieved	2
III. STATE-OF-THE-ART IN TWT EFFICIENCY TECHNIQUES AT THE START OF THE PROGRAM	2
A. Large Overvoltage Operation	3
B. Uniform Helix TWT (WJ-274)	3
C. Spent-Beam Studies	4
D. Two-Helix Tubes	5
E. Depressed Collector Operation	5
IV. EFFICIENCY AND OPERATING IMPROVEMENTS WHICH OCCURRED CONCURRENTLY WITH THE PRESENT PROGRAM	6
A. The Positive Step Taper	6
B. Uniform Long-Helix Tubes (Parameter Scaling)	7
V. THE WJ-395, A 100 WATT, HIGH EFFICIENCY TUBE	8
A. The Design Basis	8
B. Performance Characteristics of the Final Design	13
C. Physical Description	40

## LIST OF ILLUSTRATIONS

<u>Figure Number</u>	<u>Title</u>	<u>Page Number</u>
1	Power output, saturation gain and overall efficiency versus frequency of WJ-395 S/N 14.	14
2	Reproduction of Final Data Sheet of WJ-395 S/N 14.	16
3	Power output, saturation gain, and beam efficiency versus helix voltage for WJ-395 S/N 14.	17
4	Transfer curves of WJ-395 S/N 14 showing effect on saturation region of different helix voltages.	18
5	Transfer curve of WJ-395 S/N 14 at maximum efficiency conditions.	20
6	Transfer curve of WJ-395 S/N 14 at reduced efficiency conditions.	21
7	Transfer curve and helix current of WJ-395 S/N 14 for various operating conditions.	22
8	Transfer curve and helix current of WJ-395 S/N 14 for various operating conditions.	23
9	Transfer curve and helix current of WJ-395 S/N 14 for various operating conditions.	24
10	Overall efficiency and dc power input versus RF power output for WJ-395 S/N 14 showing variable-power characteristics.	26
11	Variable-power voltage program for anode, helix and collector of WJ-395 S/N 14 as a function of RF power output.	27

List of Illustrations (Continued)

<u>Figure Number</u>	<u>Title</u>	<u>Page Number</u>
12	Comparison of measured and computed small signal gain characteristics versus helix voltage of WJ-395 S/N 14.	29
13	Input VSWR of WJ-395 S/N 14 under operating and non-operating conditions.	31
14	Plot of power output and load VSWR versus position (or phase) of load discontinuity of WJ-395 S/N 14.	32
15	Noise power density versus frequency with a saturated carrier at 2.295 GHz.	34
16	Photograph of a WJ-395 tube which is prepared for preliminary test.	41
17	Photograph of WJ-395 S/N 14 after encapsulation.	42
18	Outline Drawing of WJ-395.	43

## TABLE OF TABLES

<u>Table Number</u>	<u>Title</u>	<u>Page Number</u>
I	TWT Design Parameters and Helix Diagram	12
II	Temperature Test of WJ-395 S/N 10 Encapsulated Tube	36
III	Vibration Tests of WJ-395 S/N 10 Encapsulated Tube	37
IV	Shock and Acceleration Tests of WJ-395 S/N 10	38

## I. PURPOSE OF THE DEVELOPMENT PROGRAM

This final report describes a traveling-wave tube designed to meet advanced requirements of deep space probe communication systems during the 1970 decade. It is capable of generating 100 watts of CW RF power output at an overall efficiency of 50 percent. It is also designed using a cathode technology capable of giving 50,000 hours or more of operating life.

The purpose of developing a tube of these characteristics, far in advance of its actual requirement, is based upon the sound premise that to prove out a tube and system with long life and reliability requirements, it is necessary to begin meaningful life test programs many years in advance of the launch date. The Spacecraft Radio Development Group of the Jet Propulsion Laboratory had the foresight to anticipate this need, and development of this tube was begun slightly over two years ago with goals which represented a real advance in high efficiency technology for practical space hardware. The program has been successful and high performance characteristics have been reached.

## II. GOALS AND ACHIEVEMENTS

### A. Goals Established for this Development

The following list of design goals represents the major performance goals established for this program. The detailed design specification is given in JPL Specification GMY-50467-DSN.

Frequency Range	2295 $\pm$ 15 MHz
Power Output	100 watts min.
Overall Efficiency, including heater power	55 percent
Saturation Gain	30 dB min.
Focusing	PPM (Periodic Permanent Magnet)
Cooling	Conduction only
Weight	7 pounds max.

#### Environment:

Shock	200 g, 1.0 ms terminal peak sawtooth
Vibration	14 g rms random
Temperature	-20 to +75°C
Thermal-Vacuum	10 <sup>-4</sup> Torr

#### B. Performance Achieved

Frequency Range	2295 ±15 MHz
Power Output	103 watts min.
Overall Efficiency, including heater power	50.5 percent bandcenter
Saturation Gain	38 dB
Focusing	PPM
Cooling	Conduction only
Weight	2.50 pounds
Environment	Meets shock, vibration and temperature. Not yet finally tested in high vacuum.

### III. STATE-OF-THE-ART IN TWT EFFICIENCY TECHNIQUES AT THE START OF THE PROGRAM

At the beginning of this program, the state-of-the-art in traveling-wave tube efficiency had progressed to the point where PPM focused space type tubes had given 33 percent beam efficiency and 40 percent overall efficiency. Actual production flight tubes yielded in the order of 34 percent overall efficiency. Laboratory tubes, focused in solenoidal magnetic fields had demonstrated more than 40 percent beam efficiency. Through the use of specially designed current and velocity analyzers, measurements on the spent beams emerging from these tubes indicated that a collector could be depressed to give an overall efficiency greater than 50 percent.



#### A. Large Overvoltage Operation

Efficiency improvement has largely come about by overvoltage operation of the TWT. This means that the beam voltage applied to the tube is a value much larger than that which gives maximum small signal gain. The beam velocity which is controlled by the beam voltage is adjusted to the point where small signal gain drops to a value almost zero. When the tube is designed with sufficient length between the attenuator and the output end of the tube and is driven into the large signal region, a large and rapid growth of the signal takes place near the end of the tube. With the correct choice of parameters, large values of beam efficiency can be achieved.

The performance characteristics of a tube operating under large overvoltage conditions show very little small signal gain. Near saturation drive there is a very abrupt increase in power output for a small change in input RF drive power (as much as 20 dB increase in output for a 5 dB change in input). The saturation region may be several dB wide in drive power. Because this type of performance involves a beating-wave type of interaction, electrical lengths of the helix become critical and the operating bandwidth becomes relatively narrow compared to normal broadband TWT operation.

#### B. Uniform Helix TWT (WJ-274)

The first tube to embody the large overvoltage concept and reduce it to practice in real space hardware was the WJ-274, a 20 watt, 2.3 GHz TWT.<sup>1\*</sup> This was a uniform pitch helix tube which used the same pitch helix in the input and output section of the tube. Approximately one-third of the helix was ahead of the attenuator and two-thirds of the helix followed the attenuator. It is a metal-ceramic tube using direct connection transitions from helix to the external coaxial transmission system.

The best performance of such a design was 36 percent beam efficiency and 40 percent overall efficiency (including heater), under voltage and current conditions which give maximum efficiency. The saturation gain of the tube,

---

\* This work was sponsored by the National Aeronautics and Space Administration, Langley Research Center, under Contract No. NAS1-3766 and NAS1-5923.

with the helix characteristics given above, is 20 dB. The power output of this design at the maximum efficiency conditions was 35 watts. Higher gain versions of this tube were later made and delivered for actual space systems. The higher gain was achieved by designing the input helix section with a different pitch so that it would operate closer to synchronism. Gain values of 36 dB were achieved.

### C. Spent Beam Studies

Watkins-Johnson has undertaken a series of research programs to discover new methods for improving TWT efficiency. \* The early part of this program was spent in examining the electron beams emerging from the helix of a TWT under all combinations of operating conditions. This was done with velocity and current analyzer system operated at a fundamental frequency of 1000 MHz. The analyzers worked to a frequency of 5000 MHz and used a sampling oscilloscope system for display. In this manner they were able to measure up to the 5th harmonic of the fundamental frequency in the beam. An accurate picture of the bunched current waveform in the beam could be displayed. <sup>2</sup> With the analyzers, amplitude and phase relationships between the fundamental current component in the beam and the fundamental voltage waveform on the helix could be established.

One result of these studies was the recognition that less than 50 percent of the fundamental energy content of the bunched beam was being extracted by the TWT and appearing at the tube output as usable RF power. It was then determined that additional energy could be extracted by placing a cavity resonator beyond the end of the helix. Considerable RF power appeared in the cavity which was in addition to that which had already been removed by the helix. <sup>3</sup>

---

\* This work was sponsored by the U.S. Army Electronics Command (USAECOM) under Contracts DA28-043 AMC-00076 (E) and DA28-043 AMC-02004E.

The idea of placing another helix instead of a cavity beyond the first helix was conceived, the idea being that this helix could be operated at a voltage independent of the first helix and could be driven by power from the first helix at any arbitrary phase by the use of a phase shifter between sections. In this way, the idea of the two-helix tubes evolved.

#### D. Two-Helix Tubes

Two-helix tubes were designed, built and tested.<sup>4</sup> They allowed arbitrary operation of the second helix with respect to phase and amplitude of RF drive signal and helix voltage. Various tubes were designed with different pitch helices in the second helix section. The best of these tubes gave over 40 percent beam efficiency. The velocity distribution of the electrons in the emerging spent beam was measured by a velocity analyzer. The measurements indicated that if a depressable collector were placed on the tube, efficiency of greater than 50 percent could be achieved. Depressed collector operation was never tried.

#### E. Depressed Collector Operation

The existing state-of-the-art depressed collector at the beginning of this program must be mentioned as part of the efficiency enhancement technology. The performance of simple one and two stage collectors had been examined on a number of development programs prior to this time. It had been found that the most important design feature was to get the entire electron beam emerging from the helix into the interior of the collector body and not to allow any current to strike the edges of the entrance tunnel into the collector. This prevents direct secondary electrons from being reflected back to the helix by the electric field gradient which exists between helix and collector when the collector is depressed. Beyond this simple design criterion and the necessity for proper thermal design and distribution of heat dissipation in the collector body, the designer cannot do much to improve the performance of the collector without exotic configurations which are impractical for spacecraft use. It has been found that simple two stage collectors do not give improved performance over properly designed single stage collectors.<sup>5</sup> This is not to say that depressed collector performance cannot be improved. It is believed that some form of multistage collection employing transverse magnetic fields to prevent reflected electrons from emerging from the collector can give ultimate improvement.

The limitation on the efficiency improvement which can be obtained with the present generation of depressed collectors is determined by the reflected electrons from the interior of the collector which pass back out of the collector entrance and dissipate on the helix and the anode of the electron gun. As the collector is depressed in potential, the helix dissipation increases until its rate of dissipation increase exceeds that of dissipation decrease on the collector. At this point maximum depressed efficiency is achieved. The helix must be designed to dissipate this additional energy. Experience has shown that maximum overall efficiency of the tube is achieved when the beam efficiency is already a maximum. Additional collector depression cannot make up for the fact that the maximum energy has not already been extracted from the electron beam.

#### IV. EFFICIENCY AND OPERATING IMPROVEMENTS WHICH OCCURRED CONCURRENTLY WITH THE PRESENT PROGRAM

The present program benefitted greatly from other efficiency improvement studies which were occurring simultaneously with this program. These were both company and externally sponsored. They led to various improvements in the understanding of the controlling efficiency design parameters in addition to new techniques.

##### A. The Positive Step Taper

On the USAECOM high efficiency research program, a study was being made of the relative phase relationship of the fundamental current component of the electron beam to the fundamental voltage component propagating on the helix.<sup>6</sup> It was determined that saturation occurred when a quadrature relationship existed between the voltage and the current. In order to maintain energy extraction from the beam, it was shown necessary to keep the proper phase relationship between the current and voltage components. However, these studies showed that under large overvoltage operation, the phase of the current suddenly changed near saturation in a manner that had not been noticed before. The result was that the phase difference between the current and the voltage went quickly into the wrong quadrant and the tube quickly passed through saturation. The hypothesis was advanced that if the phase velocity of the helix waves was increased before the current phase change occurred that the proper phase relationship could be maintained over a longer period of time, allowing the extraction of more energy and thus increasing efficiency. This

idea was in direct opposition to the then current ideas of helix velocity tapering which prescribed a decrease in the helix phase velocity.

Experimental tubes were built using a discontinuous or "step" increase in velocity. This has become known as a "positive" step taper as opposed to the "negative" taper which slows down the helix waves. Beam efficiencies of greater than 40 percent were achieved with a single helix, single voltage tube.

Later versions of the tube included a depressible collector and depressed efficiencies of 50 percent were achieved. These tubes were laboratory type tubes which were focused in solenoidal magnetic fields. Their frequency ranges and power levels were also far from the current requirements, but they did provide a basis for design scaling.

An interesting characteristic of the positive taper which was not originally appreciated is its effect upon small signal gain. Large overvoltage operation suppresses small signal gain and typically has a rapid transition from small values of gain under small signal conditions to normal values of gain at saturation. However, the helix section which comprises the positive step usually has a pitch which is close to the value which gives maximum small signal gain per unit length. This short section will provide a large part of the small signal gain of the tube and has the effect of bringing the small signal gain up to near normal values. In the saturation region, its effect seems to be negligible from the gain standpoint because the average beam velocity in this helix section has shifted so far from its small signal value. Thus the same value of large signal gain is obtained as if the step were not there.

#### B. Uniform Long Helix Tubes (Parameter Scaling)

A company sponsored program was undertaken to try to identify more precisely the parameters which controlled high efficiency and to provide better information for scaling to other frequency and power ranges. The tube design was changed to allow body construction techniques more closely akin to PPM focused TWT's. The ratio of the barrel inside diameter to the mean helix diameter was chosen to correspond to a typical PPM tube. Uniform helices of accurately known dimensions and pitch were used so that scaling information would be accurate. Tubes were built with the same pitch helices throughout the entire length. These were also solenoid focused tubes.

As accurate and complete electrical and RF measurements as possible were made. Characteristics were measured over a wide range of parameters and frequencies. It was found that a beam efficiency of 41 percent could be achieved and that under depressed collector conditions, efficiency of 51 percent could be achieved.

From the comparison of the results of positive step taper helices with uniform helices it appeared that equivalent efficiencies could be achieved. The major difference in the characteristics appears to be in the transfer characteristic, where the positive step taper tube has filled in the small signal gain region and perhaps broadened the top of the saturation region. It may also be that the design of the tapered tubes is less critical in terms of helix length, but this remains to be proven. It was shown that under these very high efficiency conditions, efficiency is a sharp function of frequency.

## V. THE WJ-395, A 100 WATT, HIGH EFFICIENCY TUBE

The WJ-395 TWT design is the result of a development program involving 15 tubes. The tube, which is PPM focused and conduction cooled, has been designed to deliver 100 watts of RF power output at 2.295 GHz into a load VSWR of 1.4:1. It has been mechanically, electrically and thermally designed to meet the requirements of launch and space environment. The best performance to date on this tube type has demonstrated 50.5 percent overall efficiency at 105 watts power output. The final delivered end item of the program, which is encapsulated to meet the environmental requirements, delivers 49 percent overall efficiency (including heater) at the 103 watt level. The tube has 38 dB of saturation gain.

### A. The Design Basis

#### 1. Large Overvoltage Operation

The tube has been designed for large overvoltage operation. The helix in the region immediately downstream from the attenuator is designed to operate at a value of the velocity parameter,  $b$ , equal to 2.90. This corresponds very closely to the point where the "three wave" calculation of small signal gain goes through a minimum. This will be described in the section on operating performance.



## 2. Gain Beyond the Attenuator

The concept of a minimum value of small signal gain following the attenuator to prevent degradation of efficiency becomes meaningless under the large overvoltage conditions. Scott<sup>7</sup> suggests that the small signal gain must be at least 26 dB to achieve maximum efficiency. But, three-wave small-signal calculations show that there is not more than 1 dB gain in the region. This is because the tube is operating under beating wave conditions and normal concepts of gain per unit length are no longer valid. Because of beating wave effects, BCN scaling is inappropriate and CN scaling is used. The small signal CN product of the output section of the tube has been chosen to be 1.44.

## 3. Use of the Positive Taper

Early tubes in the program were built with uniform pitch helices in order to establish basic electrical, thermal and mechanical design. Once this was accomplished, a number of experiments were done with positive step tapers of one and two steps and with linear positive tapers. The ultimate design uses a linear positive taper.

## 4. Use of a Synchronous Helix Ahead of Attenuator

If the tube is designed with the same pitch in the input and output helix section with approximately two-thirds of the helix following the attenuator, the saturation gain of the tube will be approximately 20 dB. It also has a characteristic of decreasing gain as a function of frequency.

To achieve the minimum of 30 dB saturation gain required by the specifications, the input helix design has been shifted to correspond to a phase velocity which will give approximately maximum small signal gain per unit length at the operating helix voltage. Experiments have shown that the total saturation gain of the tube can be adjusted to any arbitrary value by adjusting the small signal gain ahead of the attenuator. It has been determined that gain adjustments made in this way do not affect efficiency.

There are two side benefits from the synchronous input helix section. The first is that this section of helix has an increasing gain characteristic vs. frequency. This just compensates for the decreasing saturation

gain vs. frequency of the output helix section and gives an overall flat characteristic vs. frequency. Secondly, for "variable-power" operation which will be described later, the synchronous helix section has an increasing gain characteristic with increasing beam current and helix voltage. The rate of gain increase can be made to just match the rate of power output increase at optimum variable-power current and voltage conditions. This allows the tube to operate at constant RF input drive power over a wide range of power output conditions and leads to a simplification in variable power operation.

5. Attenuator Design

The attenuator design criteria is extremely simple: design for minimum length. The length of the attenuator on the final tubes was 0.2 of the reduced plasma wavelength in the beam. The short length minimizes large signal effects upon the beam efficiency of the tube due to the beam drifting through the attenuator. Greater than 50 dB of attenuation is realizable with this attenuator length without using a physical sever in the helix.

6. Collector Depression

At maximum efficiency, experience has shown that the collector voltage will depress to 0.7 of the helix voltage. Variations in collector design have shown very little effect upon this value. The collector entrance tunnel diameter was chosen sufficiently large so that no current would be intercepted on it under any combination of currents and voltages.

7. Electron Beam Formation

The electron beam is produced by a conventional Pierce type convergent flow electron gun with an area convergence of 33.6. At the nominal beam current of 110 mA, the cathode current density is 245 mA/cm<sup>2</sup>. The cathode material chosen is high purity 0.15 percent zirconium cathode nickel. This is operated at a true temperature of 740°C. Under these conditions, 90 percent depletion of the cathode coating should occur at 50,000 hours. To prevent foreshortening of cathode life by

ion bombardment of the cathode, an ion block is built into the electron gun by the simple expedient of designing the gun to operate with the anode voltage greater than helix voltage.

Under small signal conditions, the beam diameter is that predicted by the Brillouin equilibrium diameter for the rms value of magnetic field, beam current and effective space-charge-depressed-beam potential. The beam diameter, which has been verified by small signal gain calculations, is 0.4 of the mean helix diameter.

#### 8. PPM Focusing

The PPM focusing magnet stack is composed of 45 cells of Alnico 8 magnets and 9 cells of Platinum-Cobalt magnets. The Alnico 8 magnets are over the small signal section of the tube and use a plasma wavelength to magnet period ratio of 2.68. The Platinum-Cobalt material is over the large signal section of the tube and uses a plasma wavelength to magnet period ratio of 3.30. The platinum-cobalt is necessary to maintain the same value of peak magnetic field (850 gauss) in the shorter period section at the end of the tube. The magnetization of the individual cells of the stack are programmed to maintain a uniform peak magnetic field over the entire length of the tube.

Incomplete tests tend to indicate the focusing could be maintained with the longer period magnets used over the entire length of the tube. Thus the Alnico V platinum-cobalt hybrid stack could be replaced with an all Alnico stack. Comparison of all details of focusing under various values of RF drive and helix voltage must be made before a final decision can be made to use only one period. This has not been done as of this time.

#### 9. TWT Design Parameters

Table I lists the TWT design parameters which correspond to the frequency of maximum efficiency. The helix diagram shows the lengths and TPI's of the helix and attenuator sections. The parameters are the standard TWT design parameters based upon Pierce<sup>8</sup>.

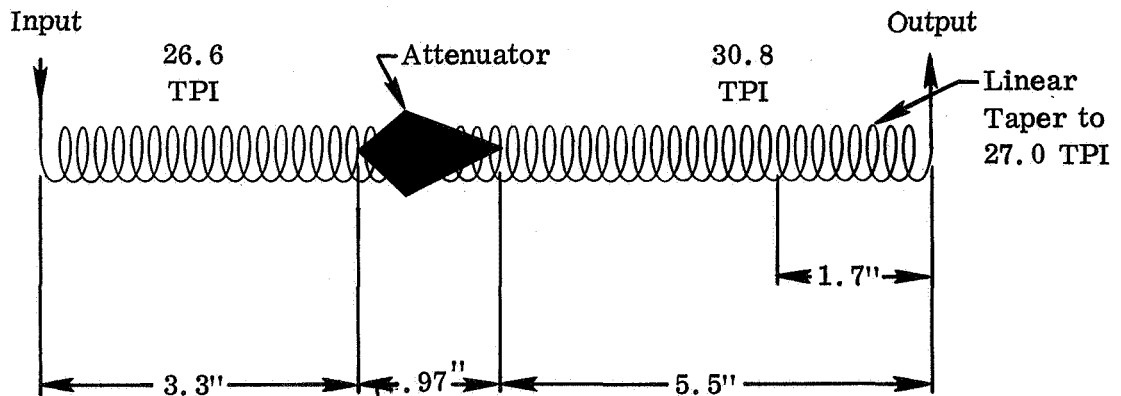
TABLE I

## TWT DESIGN PARAMETERS AND HELIX DIAGRAM

$$f_0 = 2.295 \text{ GHz}$$

(Frequency of Maximum Efficiency)

<u>Parameters (Ref 8)</u>	<u>26.6 TPI Section</u>	<u>30.8 TPI Section</u>
Beam Perveance ( $\mu\text{pervs}$ )	.83	.83
$\gamma_a$ , Helix circumference meas. in guide wavelengths	.886	1.03
C, Gain Parameter	.102	.104
QC, Space Charge Parameter	.221	.210
d, Loss Parameter	.043	.044
b, Velocity parameter	1.20	2.90
b/a, Beam to mean helix radius	.40	.40
CN of output section	--	1.44
BCN of input section	26.4 dB	--



## B. Performance Characteristics of the Final Design

The performance curves which are shown in the following section are those measured on WJ-395 S/N 14. This helix design has produced the best efficiency performance of all the experimental designs constructed on this program. The data represented here were measured on the tube in its final encapsulated form and is an indication of real performance that can be achieved on a deliverable tube. Better efficiency performance was realized from the tube before encapsulation while it could be operated under optimum focusing conditions on the laboratory test stand. Under these ideal conditions, an overall efficiency of 50.5 percent at a power output of 105 watts was measured at a frequency of 2295 MHz.

When high efficiency performance such as that described in this report is measured, extreme care must be taken in the measurement procedures used. The RF power measurements are made with a power measuring system which has been accurately calibrated against a calorimetric standard. Voltages and currents are measured with precision instruments which are directly traceable to accurate standards. Even the heater power to the tube is supplied from a dc source to allow the accurate measurement of voltage and current with dc instruments to avoid waveform errors that can occur with ac instruments. The data presented are as accurate as can be reasonably determined with modern RF and dc measuring techniques.

### 1. Power Output, Saturation Gain and Overall Efficiency vs. Frequency

Curves which show power output, saturation gain and overall efficiency vs. frequency are plotted in Fig. 1. These are shown for a beam current of 110 mA and for three different values of helix voltage. The optimum efficiency performance of 49 percent at the design frequency is obtained with a helix voltage of 2600 volts. When the optimum helix voltage is applied, it is seen that the efficiency curve is peaked. This is a very expanded scale, however, and efficiency is seen to vary less than 1 percent over a 75 MHz range. Under the 2600 volt conditions, power output remains above 100 watts over a 140 MHz range. Saturation gain varies less than  $\pm 0.2$  dB over the same 140 MHz range. The overall efficiency remains above 40 percent under fixed operating conditions over a frequency range from 2050 MHz to 2480 MHz.

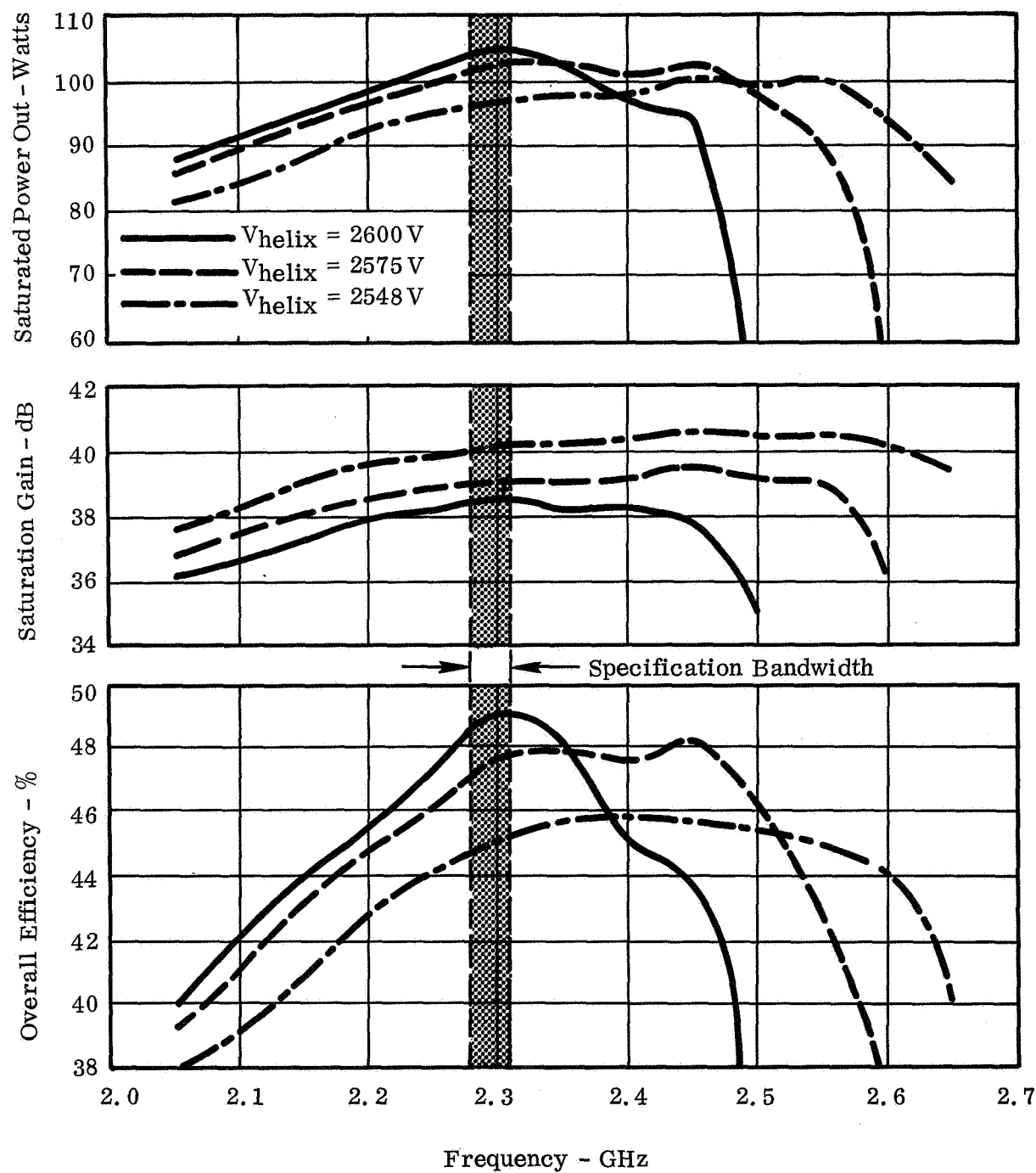


Fig. 1 - Power output, saturation gain and overall efficiency vs. frequency of WJ-395 S/N 14. Beam current = 109.8 mA.



If the helix voltage is decreased by approximately 1 percent, peak overall efficiency decreases by 1 percent but the bandwidth for a 1 percent change in efficiency increases to 200 MHz. The band center shifts upward in frequency by 75 MHz. Further reduction in helix voltage reduces the peak efficiency further but also leads to wider band operation.

A more detailed set of data for closer frequency intervals is shown in Fig. 2 which is a reproduction of the final data sheet of WJ-395 S/N 14.

2. Beam Efficiency, Saturation Gain and Power Output vs. Helix Voltage

Figure 3 shows the characteristics which have become the basic characteristics for evaluating the performance of a tube. These plots are shown for the specification frequency of 2295 MHz and show saturation power output, saturation gain and beam efficiency as a function of helix voltage with beam current as the parameter. Keep in mind that this efficiency does not include the efficiency enhancement effects of depressed collector operation. It is seen that the peak efficiency increases with increasing beam current until at 112 mA and 2600 volts the maximum beam efficiency of 37 percent has been reached. At higher current, the peak efficiency begins to drop.

The almost linear rise of beam efficiency with helix voltage at a fixed value of current is a consequence of increasing overvoltage operation. The sudden drop of beam efficiency just beyond the peak efficiency point occurs because the beam is becoming nonlinear in the attenuator region. When this condition occurs, beam efficiency plunges rapidly.

3. Transfer Characteristics

The power transfer characteristics (power output vs. power input) is perhaps the most useful curve to the system designer. It gives the allowed variation of drive power to achieve any specified range of output power variation. Fig. 4 shows a set of these curves at the fixed current of 110 mA with helix voltage as the parameter. It is seen that a drive power variation of  $\pm 2.0$  dB just gives a power output variation of 1.0 dB on the 2600 volt curve. This just meets the specification power

FINAL DATA SHEET  
 WJ-395 SERIAL NUMBER 14

Frequency (GHz)	Power Input (dBm)	Power Output (dBm)	Power Output (Watts)	Anode Current (mA)	Helix Current (mA)	Gain (dB)	Overall Efficiency (%)
2.2650	12.0	50.15	103.5	.56	13.5	38.15	47.9
2.2725	12.0	50.15	103.5	.57	13.5	38.15	47.9
2.2800	12.0	50.18	104.0	.56	13.2	38.18	48.30
2.2875	12.0	50.20	105.0	.50	12.7	38.20	49.02
2.2950	12.0	50.20	105.0	.50	12.5	38.20	49.02
2.3025	12.0	50.20	105.0	.52	12.5	38.20	49.02
2.3100	12.0	50.20	105.0	.52	12.0	38.20	49.10
2.3175	12.0	50.18	104.0	.46	11.6	38.18	48.60
2.3250	12.0	50.15	103.5	.52	11.6	38.15	48.50

Beam Current = 109.8 mA

Heater Current = 0.83 A

All Voltages Referenced to Cathode

Lead Color Code

Anode = 3275  
 Helix = 2600  
 Collector = 1830  
 Heater = 4.3 d.c.

Anode - Green  
 Helix - Orange (Capsule Ground)  
 Collector - Red  
 Heater-Cathode - Yellow  
 Heater - Brown

Current, no RF applied  
 Helix = 1.0 mA  
 Anode = 0.1 mA  
 Collector = 108.7 mA

Weight: 2.345 lbs.

19 August 1968  
 Tom Bobo, Technician

Fig. 2 - Reproduction of Final Data Sheet of WJ-395 S/N 14.

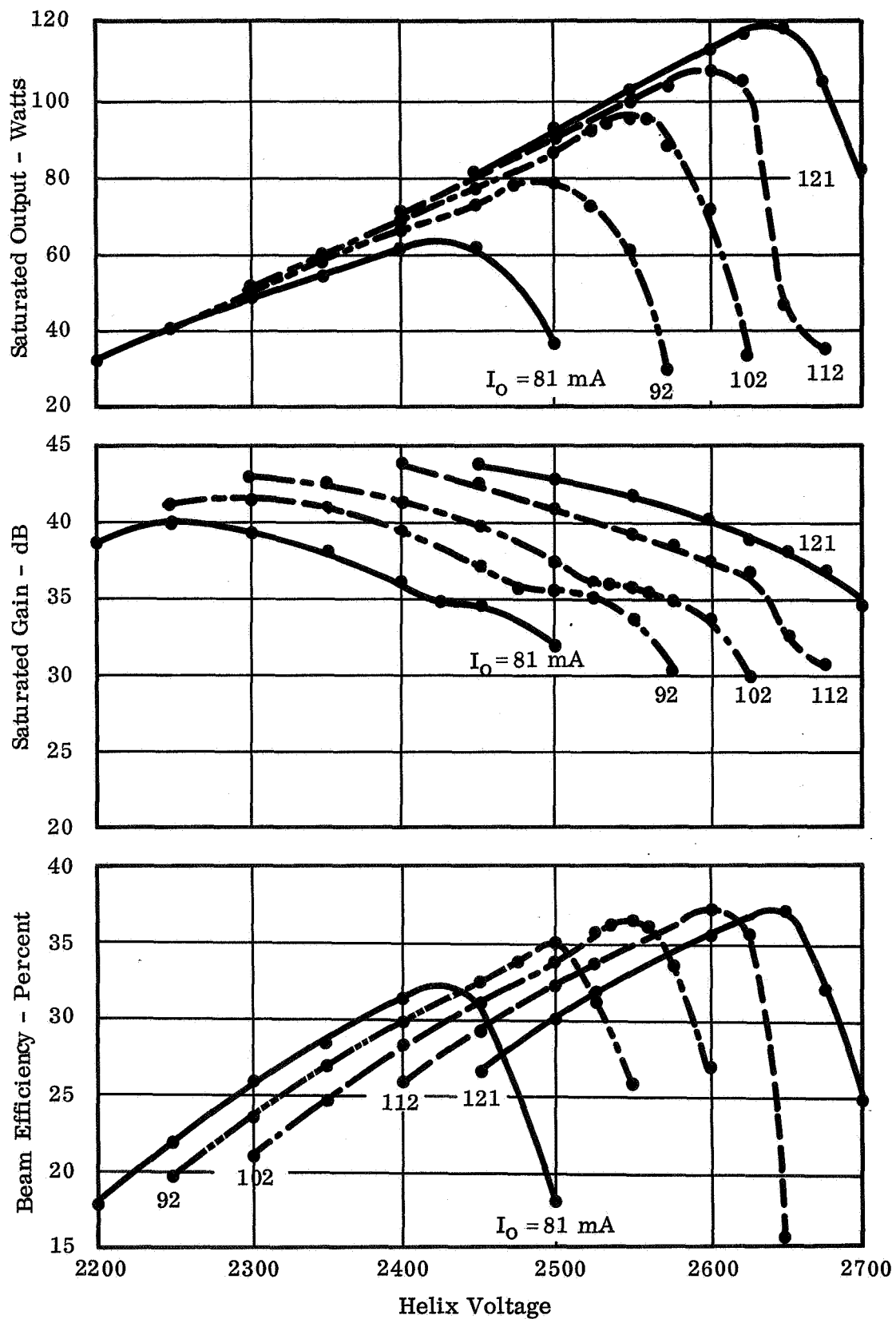


Fig. 3 - Power output, saturation gain, and beam efficiency vs. helix voltage for WJ-395 S/N 14. Frequency is 2.295 GHz.

19174A

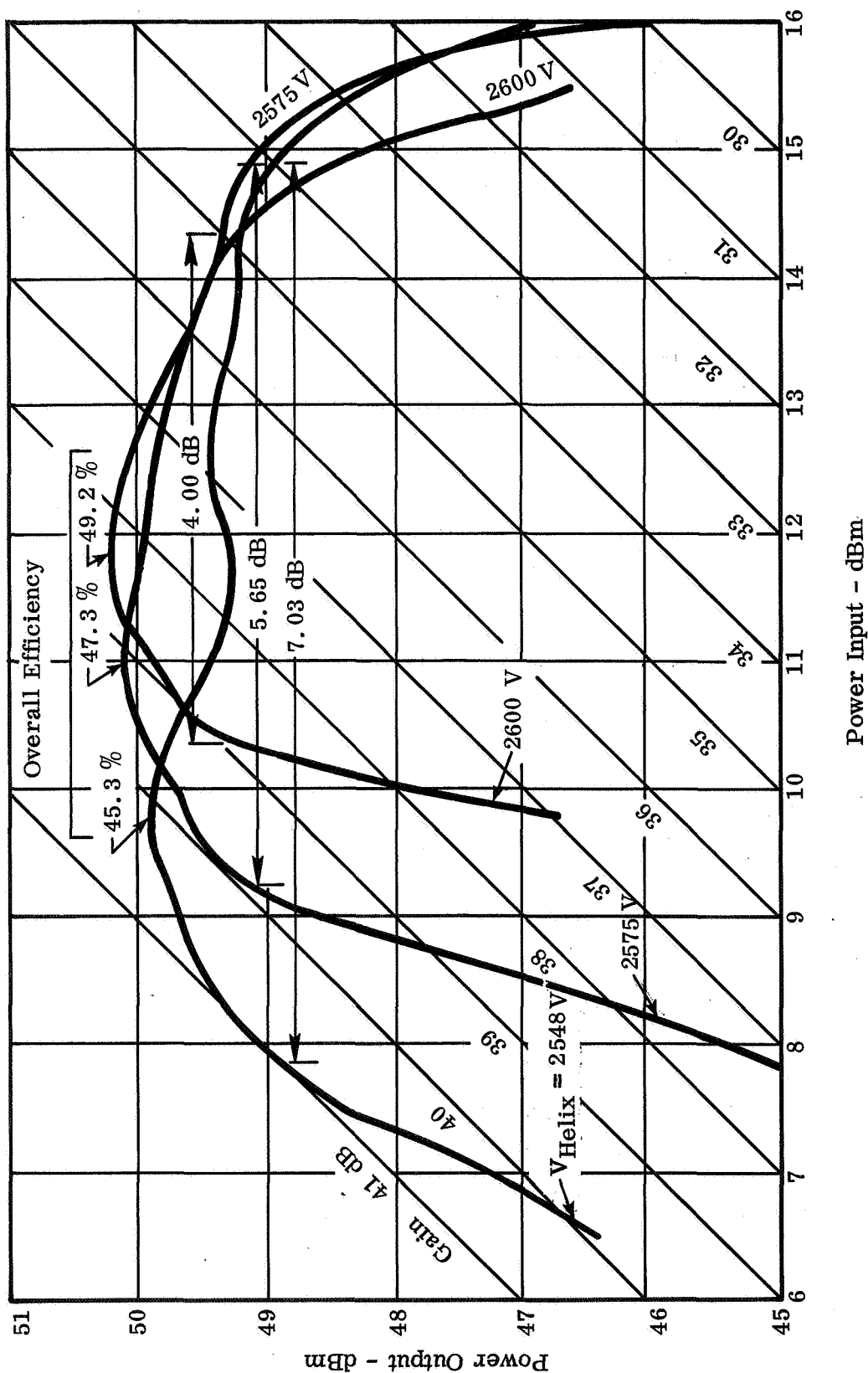


Fig. 4 - Transfer curves of WJ-395 S/N 14 showing effect on saturation region of different helix voltages. Frequency = 2.295 GHz. Beam current = 109.8 mA. Collector voltage = 1830 volts. Drive range widths shown are for 1.0 dB variation in power output.

variation requirement. This curve has a peak efficiency of 49.2 percent. If, however, the peak efficiency requirement is relaxed by 2 percent to 47 percent, the allowable drive power range for a 1.0 dB output variation has increased to 5.65 dB. For an efficiency relaxation to 45 percent, the allowable drive power range becomes 7.0 dB.

An idea of the amount of AM that would be generated as a function of helix voltage ripple can be estimated by power output variation as a function of helix voltage at a fixed value of RF input power.

Figure 4 represents data taken in the region of saturation. The transfer characteristic viewed on a wider range of input and output signal levels has some interesting aspects. Figure 5 shows that the small signal gain is 27 dB. At about 6 dB below saturation drive, the power output starts to climb very steeply and increases by about 20 dB before reaching saturation. This very rapid rise in power output is typical of large over-voltage operation. The small signal range is of little interest to the user who requires high efficiency, but is shown to give an overall picture of the characteristic.

Figure 6 shows the same characteristic under the operating conditions corresponding to 45 percent overall efficiency. It is seen that the rise in signal output with drive is less abrupt and the broader top on the curve can be seen.

Figures 7, 8, and 9 show a repeat of the transfer curves under the three voltage conditions and also show the resulting helix current interception as a function of drive power and collector voltage. The 2548 volt curve (45 percent peak efficiency) shows a fairly constant value of intercepted current as a function of drive. At 2575 volts, helix current begins to rise at the low drive end, but is not excessive. At 2600 volts, there is a very pronounced peak in helix current approximately 2 dB below saturation. The peak in the current lies at a power output value which is 3.5 dB below the saturated output value and is not in a useful region of operation.

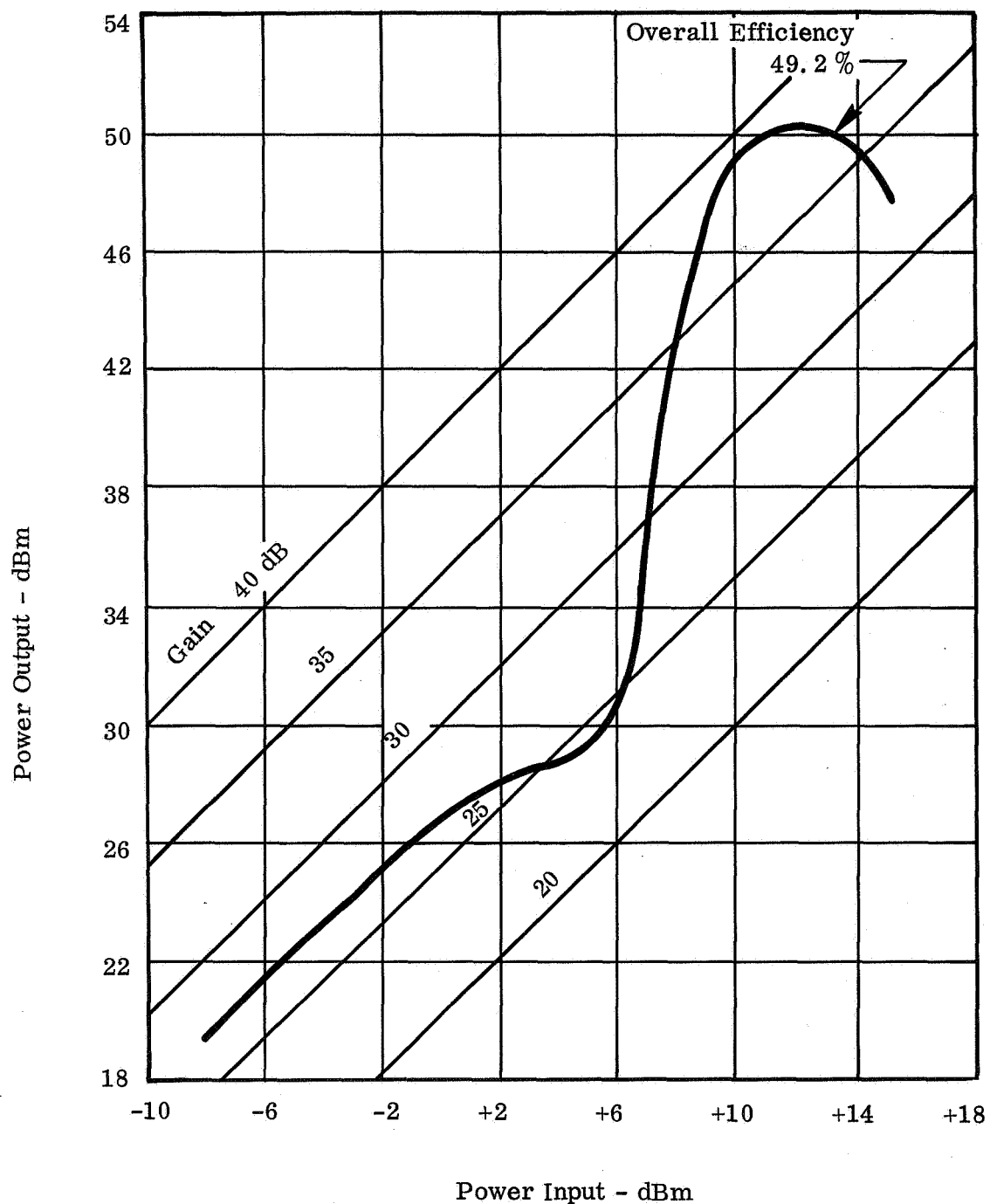


Fig. 5 - Transfer curve of WJ-395 S/N 14 at maximum efficiency conditions.  
Helix voltage = 2600 V. Beam current = 109 mA. Frequency = 2.295 GHz.



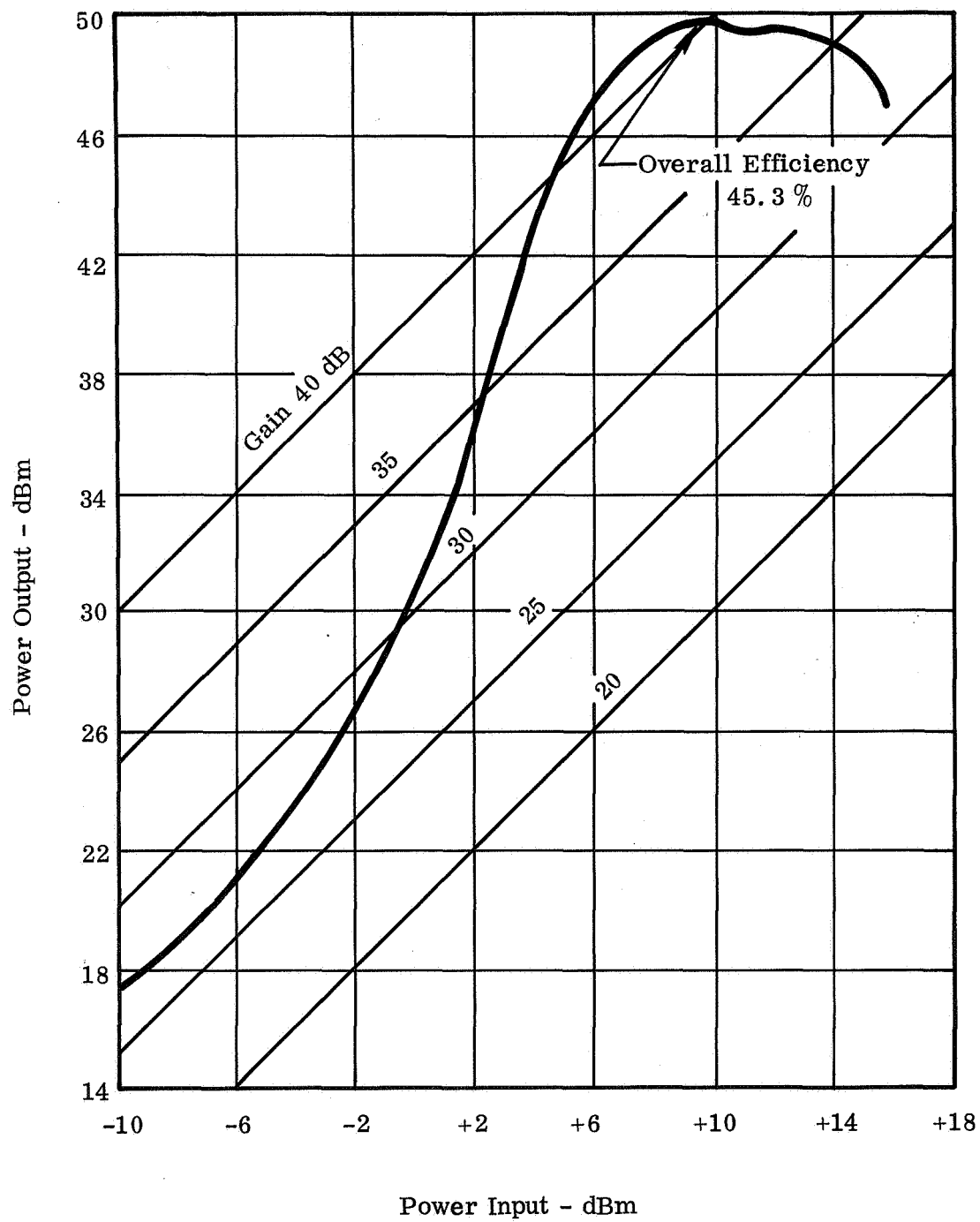


Fig. 6 - Transfer curve of WJ-395 S/N 14 at reduced efficiency conditions. Helix voltage = 2548 volts. Beam current = 109 mA. Frequency = 2.295 GHz.

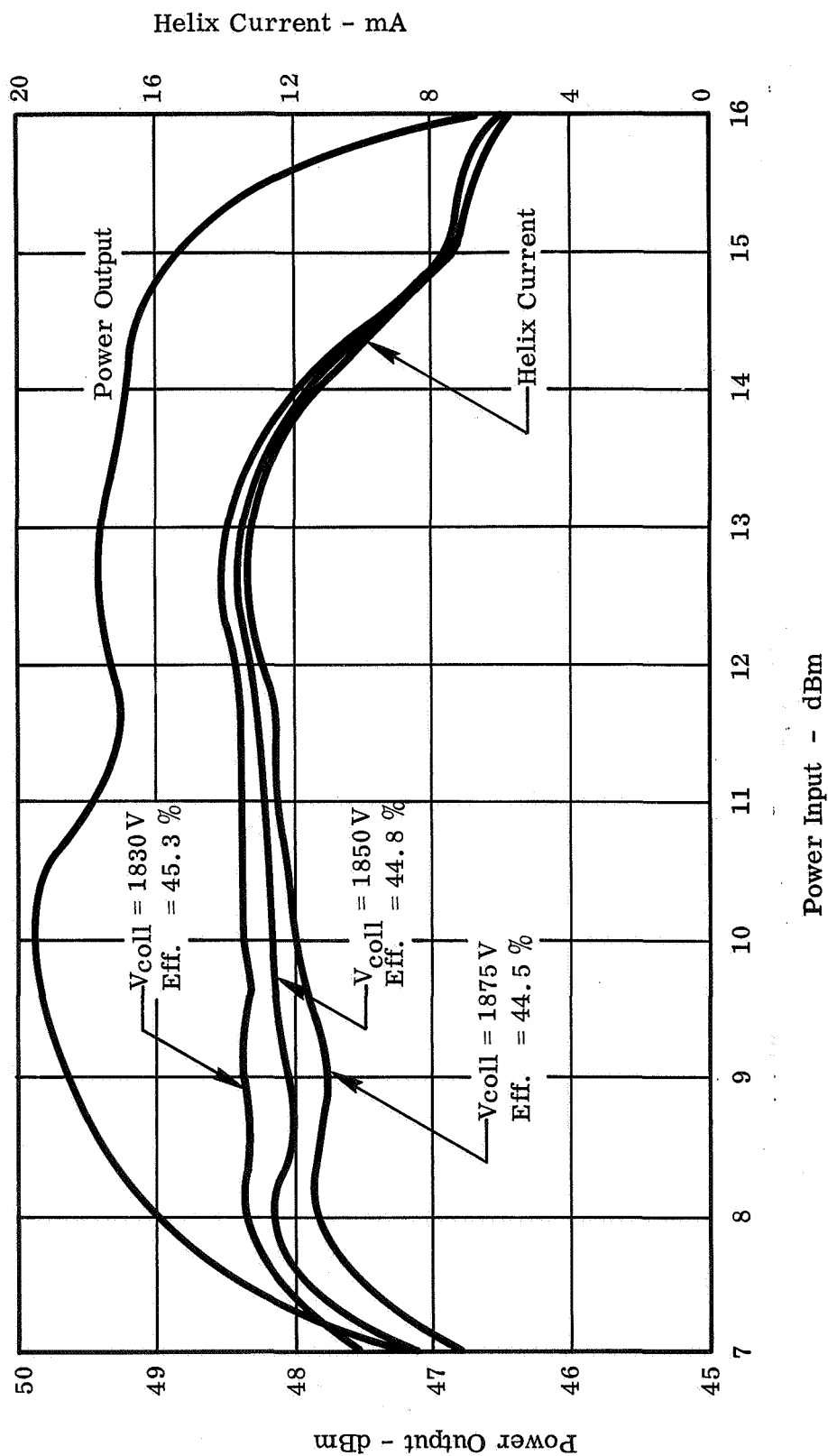


Fig. 7 - Transfer curve and helix current of WJ-395 S/N 14 for various operating conditions. Helix voltage = 2548V  
Frequency = 2295 GHz. Beam current = 109.8 mA.

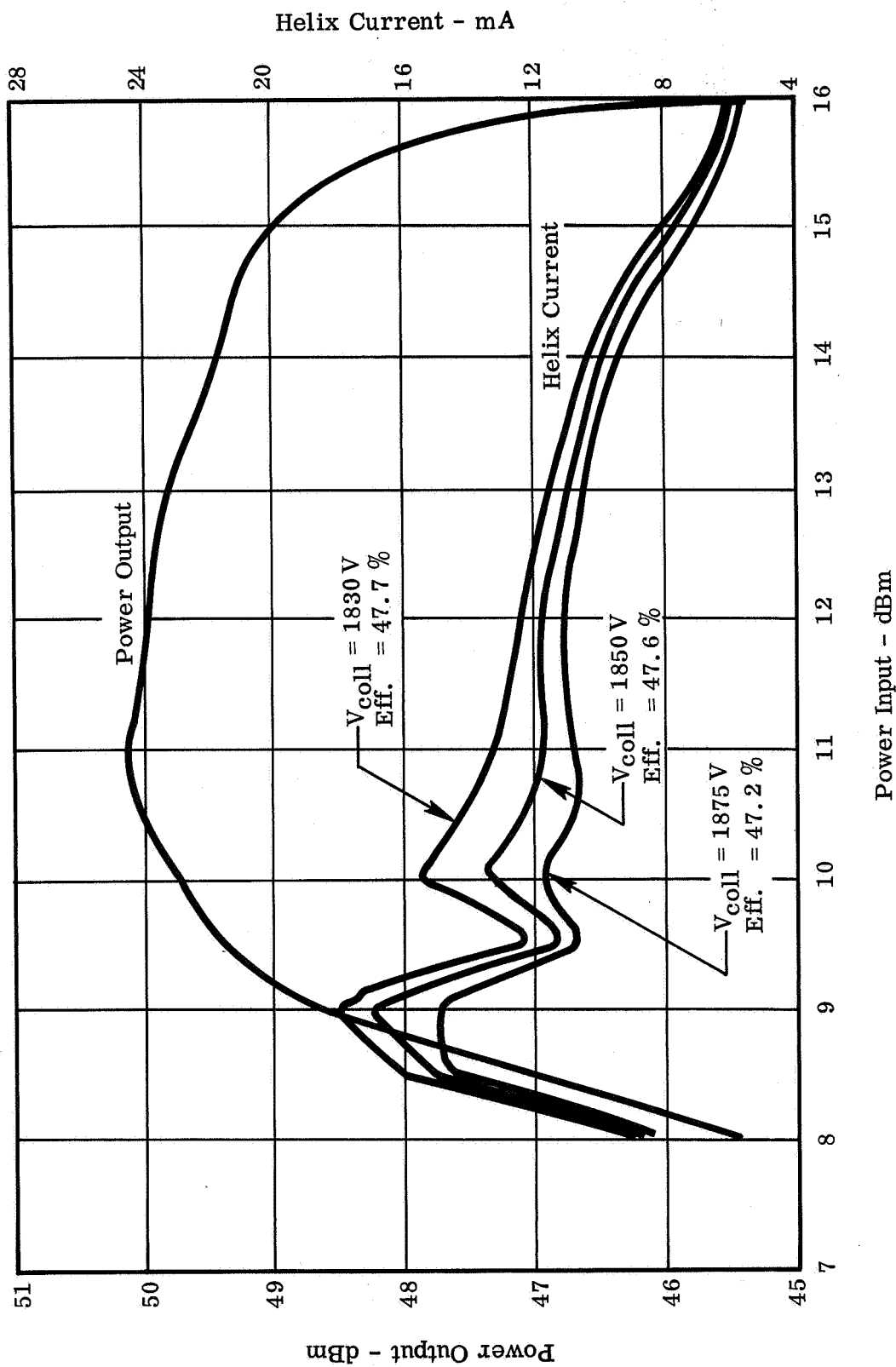


Fig. 8 - Transfer curve and helix current of WJ-395 S/N 14 for various operating conditions. Helix voltage = 2575 volts. Beam current = 109.8 mA. Frequency = 2.295 GHz.

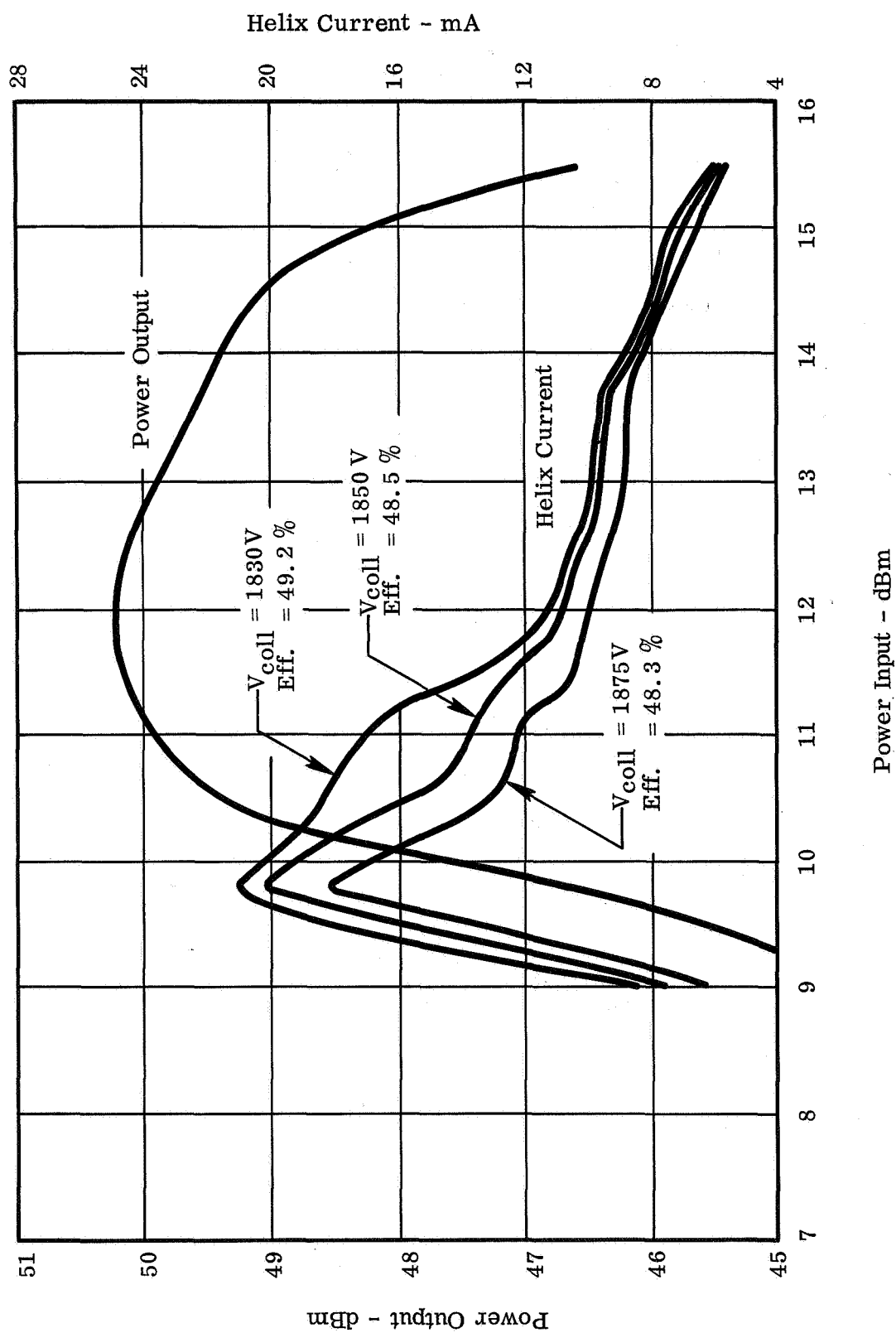


Fig. 9 - Transfer curve and helix current of WJ-395 S/N 14 for various operating conditions. Helix voltage = 2600 volts. Frequency = 2.295 GHz. Beam current = 109.8 mA.

By comparing the curves of Figs. 7, 8 and 9 one can arrive at a trade-off between peak overall efficiency, width of the drive power range, helix current interception and collector voltage. The operating conditions chosen would depend much upon the individual requirements of the system in which the tube would be used.

#### 4. Variable-Power Characteristics

Requirements often arise when it would be desirable to operate a tube at two or more power levels at different times. A typical situation might be a desire to conserve primary power under average communications requirements with the capability to go to high power operation for high data rate transmission under special circumstances. High efficiency tubes have been typically single power level devices where the efficiency deteriorates at power levels away from the design value. The WJ-395 and related tubes exhibit an interesting characteristic which has been named "variable-power, high efficiency" operation. It allows the power output of a tube to be operated over as wide a range as 10 dB in some cases while still maintaining a high overall operating efficiency. In addition, as embodied in the WJ-395, it operates with a fixed value of RF drive power and requires only that the three principal dc voltages applied to the tube be varied. Thus, varying the power output of the system becomes only a matter of programming the power supply voltages applied to the tube. In this type of operation, the tube is always working at the saturation power output and thus achieves the maximum efficiency possible at each power level.

Figure 10 shows the variable-power performance that was measured on the WJ-395 S/N 14. The upper plot shows the overall efficiency that can be obtained as a function of RF output power level. The lower plot shows the relationship between the total dc input power and the RF output power. Diagonal lines represent lines of constant overall efficiency. From this plot, the system designer can determine directly the input power required for a given output power. Maximum efficiency on this design occurs at the 100 watt level. It should be noted that this total power range (8.5 dB variation) was obtained at a fixed RF input drive level of 12.0 dBm. Even at the 18 watt level, the efficiency is greater than 31 percent. Fig. 11 shows the electrode voltages that are

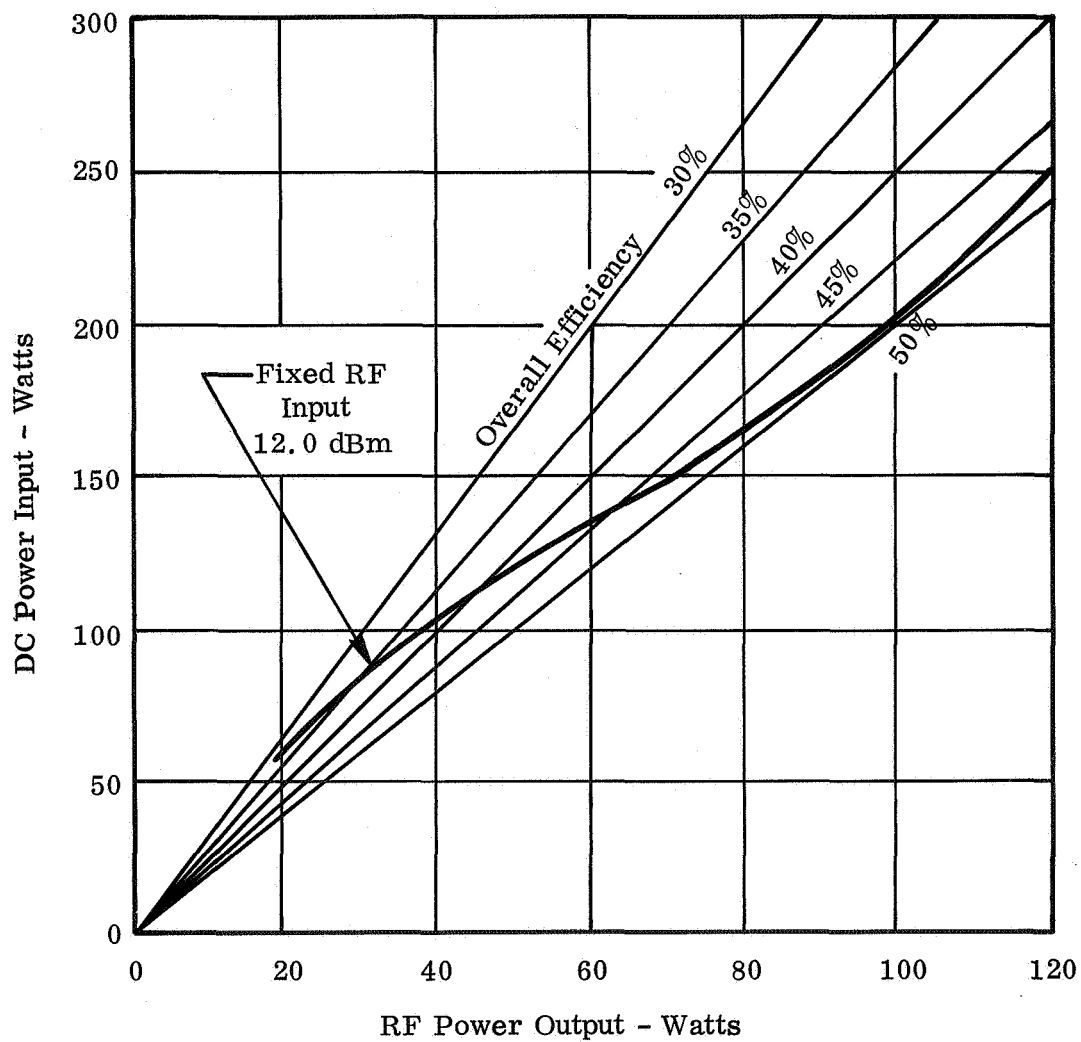
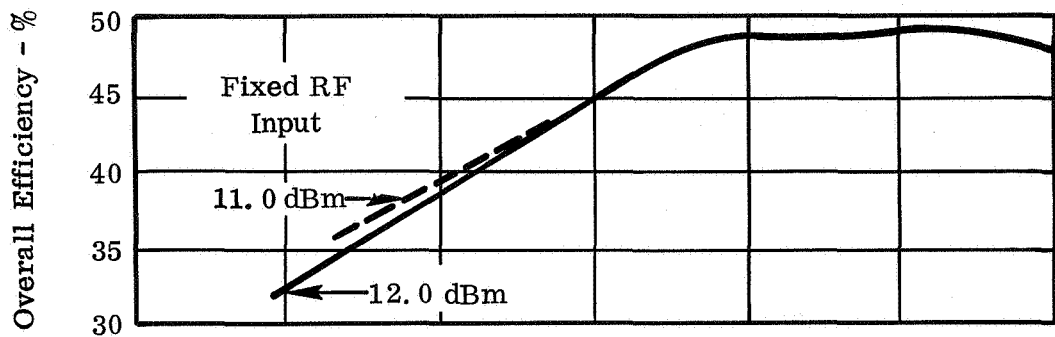


Fig. 10 - Overall efficiency and dc power input vs. RF power output for WJ-395 S/N 14 showing variable-power characteristics. Frequency = 2.295 GHz.

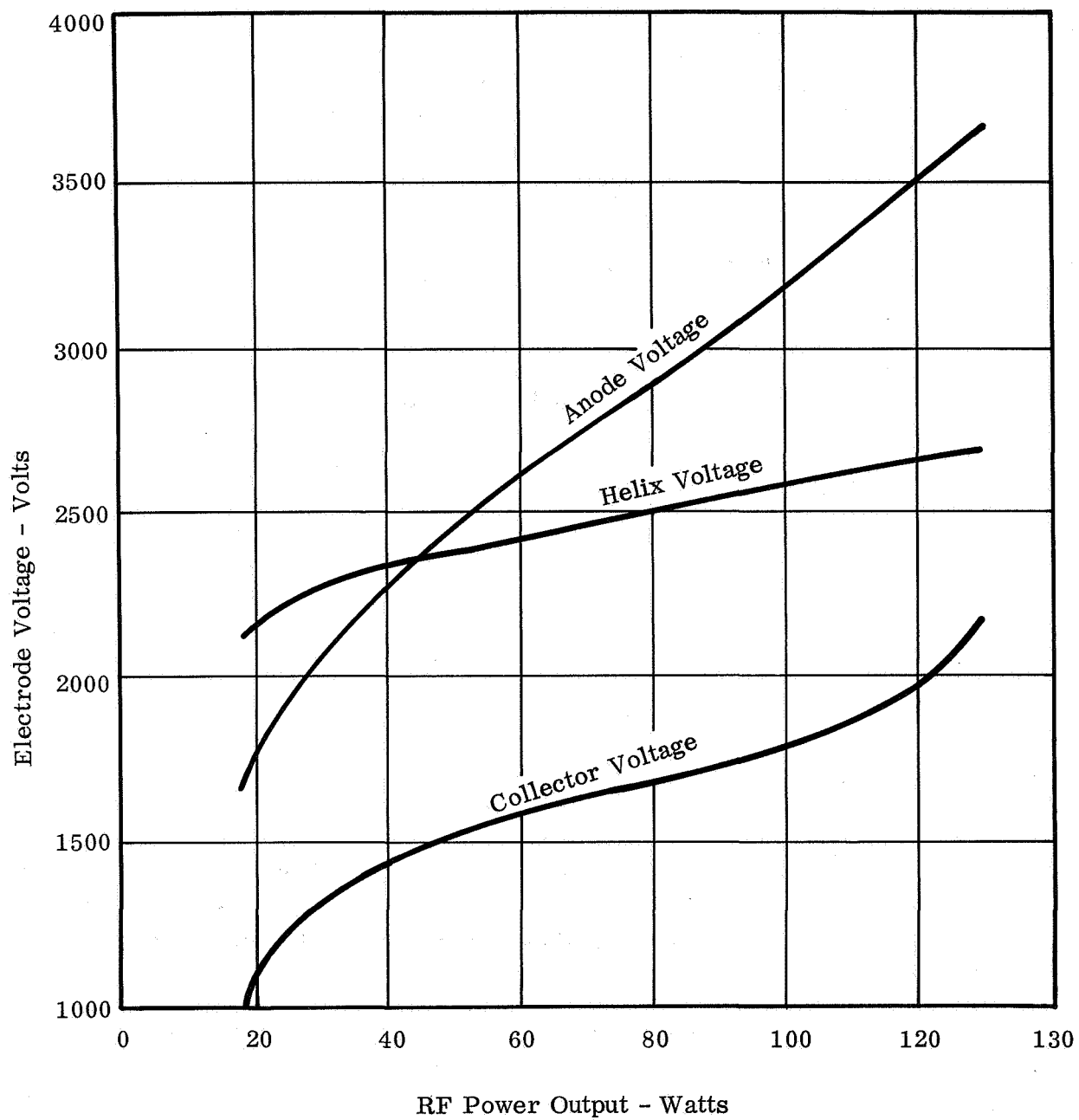


Fig. 11 - Variable-power voltage program for anode, helix and collector of WJ-395 S/N 14 as a function of RF power output. RF input to tube is fixed at 12.0 dBm.

required as a function of RF power output level. Unfortunately, the voltages are not proportional. However, power supplies have been designed, built and delivered for space system use by the Watkins-Johnson Space Communications Section of the Systems Division which are programmed for two-power-level operation.

The constant RF drive property of the tube derives from the input helix design. Because of the combined gain characteristics of the input and output helix at the optimum conditions for variable power operation, the gain increases at exactly the same rate that the power output increases. This property allows a constant drive level.

Note on Fig. 11 that the anode voltage is greater than helix voltage for all output power levels greater than 45 watts. This means that ion blocking occurs for all power levels above this value and the long life characteristics of the cathode are preserved. If the total possible variable-power range is desired, it is necessary to design the electron gun with a second anode which is always operated at a fixed voltage above the helix. This anode is located between the first anode (the current controlling electrode) and the helix. It provides an ion block under all operating conditions. Such a gun has been built and tested on the WJ-448, a tube type similar to the WJ-395 and has operated successfully.

##### 5. Correlation Between Measured and Computed Small Signal Gain

A small signal computer program has been developed at Watkins-Johnson Company to predict performance of traveling-wave tubes and to accurately determine operating parameters. The small signal program has been designed to include all known factors affecting traveling-wave tube performance including "3 wave" gain calculations and variable pitch helices so that accurate gain can be calculated even under large over-voltage operation. Small signal gain characteristics of the WJ-395 S/N 14 based upon the tube model of Table I have been calculated versus helix voltage. Measured gain characteristics of S/N 14 are compared with the calculated curve in Fig. 12. It is seen that the agreement is very close. Note that the voltage is indicated at which maximum efficiency is obtained under large signal conditions. In many different designs this voltage has occurred just beyond the minimum gain point



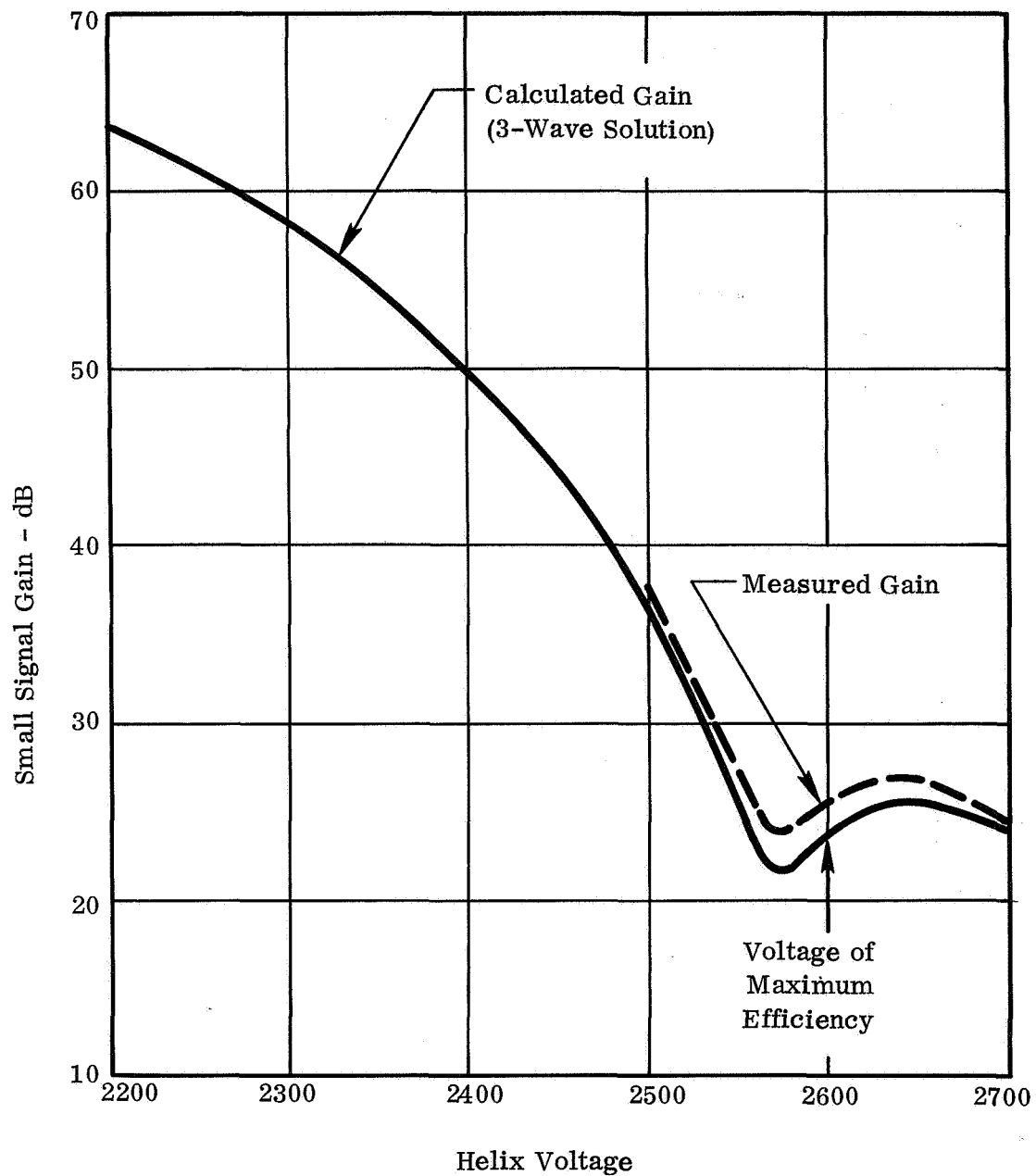


Fig. 12 - Comparison of measured and computed small signal gain characteristics vs. helix voltage of WJ-395 S/N 14. Beam current = 110 mA. Frequency = 2.295 GHz. The voltage of maximum efficiency under large signal conditions is shown.

of the "3 wave" calculation. This indicates that the high efficiency, large overvoltage operation is intimately tied into the "beating-wave" effects of the TWT.

#### 6. Operating Input VSWR

The specification requires that the operating input VSWR be less than 1.2:1. Fig. 13 shows plots of both operating and non-operating input VSWR as a function of frequency. Plots are shown for data taken when the tube was first placed into test and also the final test data. There is a large difference between the initial and final operating data. It is believed that the accuracy of both measurements was the same since the non-operating data matches very closely. The final data indicates that the VSWR is out of specification. It is believed that the initial data were taken under the same conditions, but there is no way to check that now. It seems to indicate a VSWR change during the course of the tests. This tube accumulated more than 500 hours of operation under large signal conditions during the course of testing and aging.

The large operating VSWR is due primarily to the reflection from the input side of the attenuator which becomes "visible" at the input terminal because of the large value of gain in the input section. Previous models have met the specification, but this is the first time that these data have been taken after a long operating period. This particular tube has a larger reflection coefficient at the attenuator and a higher gain in the input section than previous tubes. Both are factors which make the situation worse. The plan for future tubes is to have the input side of the attenuator modified to guarantee a more gradual transition into the attenuator.

#### 7. Effect of Load VSWR

The specifications require that the tube be able to operate into a load VSWR of 1.4:1 and maintain a minimum of 100 watts power output independent of load phase. Fig. 14 shows a plot of power output vs. position of the load discontinuity at the standard operating conditions. The position of the load discontinuity controls the phase of the reflection presented by the load to the tube. It was very difficult to obtain a

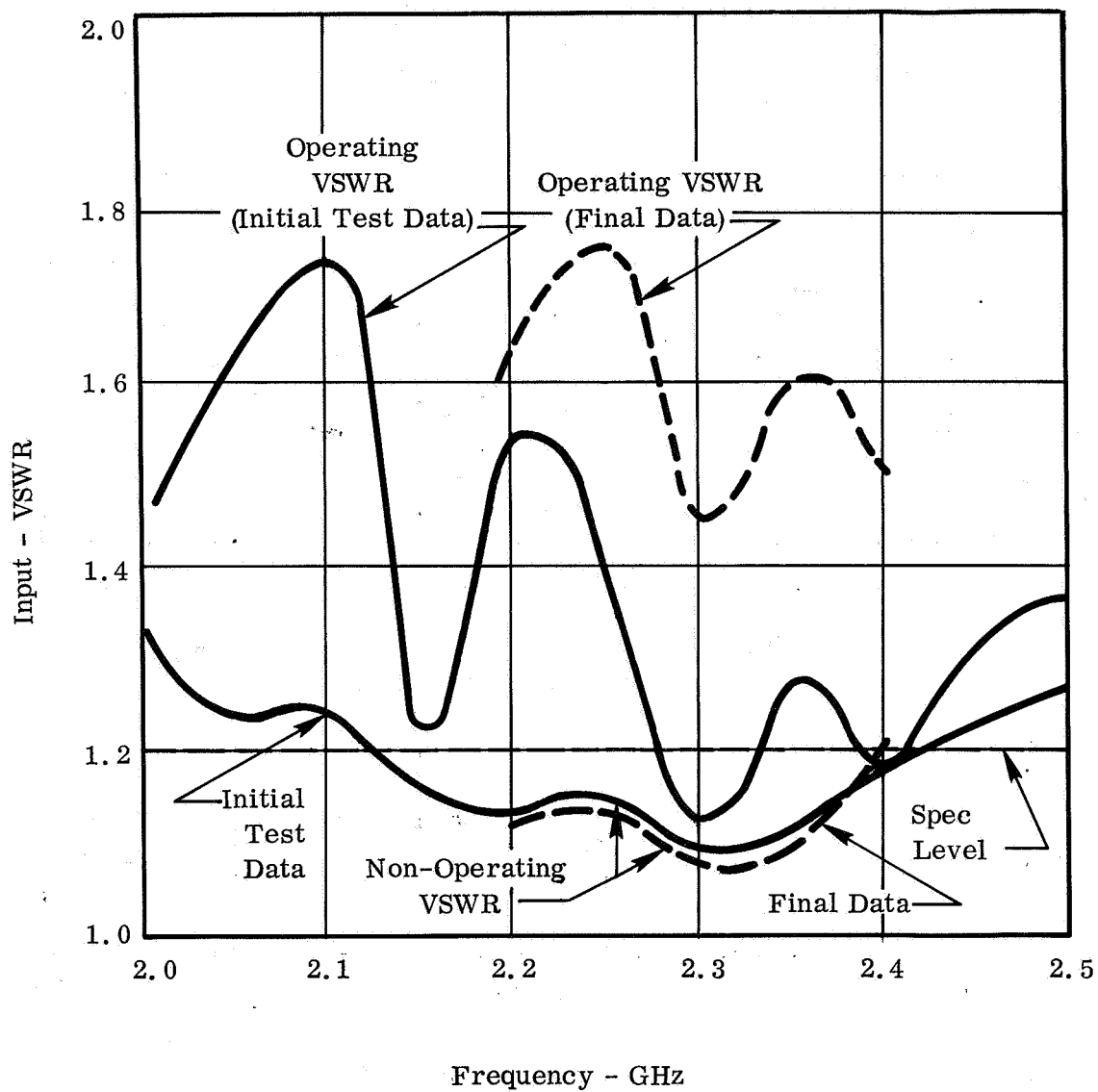


Fig. 13 - Input VSWR of WJ-395 S/N 14 under operating and non-operating conditions. Helix voltage = 2600 volts. Beam current = 110 mA.

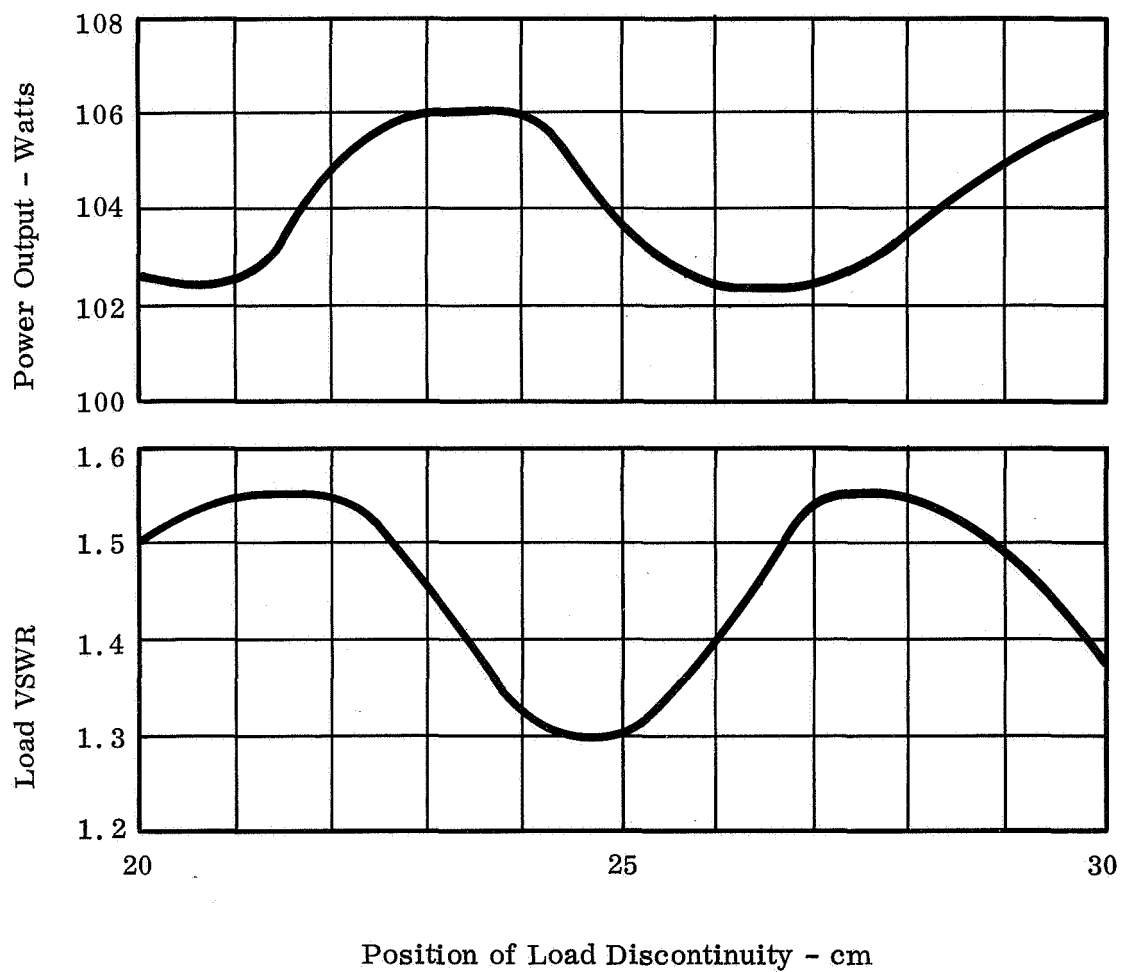


Fig. 14 - Plot of power output and load VSWR vs. position (or phase) of load discontinuity of WJ-395 S/N 14. Helix voltage = 2600 volts. Beam current = 110 mA. Frequency = 2.295 GHz.

variable-phase load which could present a constant VSWR with a 100 watt power handling capability. The VSWR vs. discontinuity position shown in Fig. 14 is the best that could be presented to the output terminal of the tube under the operating limitations of the measuring system. It is seen that the power output remained greater than 102 watts for all phase conditions. The phase was varied over more than  $180^{\circ}$ .

#### 8. Output Noise Power Density

The noise generated by the tube at frequencies away from the carrier is important to spacecraft system design. Fig. 15 shows the noise power density vs. frequency over the range from 2.0 to 2.5 GHz with the tube operating under saturated conditions at the 100 watt level. It is seen that noise density is fairly flat vs. frequency. The gap in the curve represents the region where the receiver skirt selectivity cannot reject the carrier signal. Noise close to the carrier could not be measured with this system.

At drive levels below saturation, the noise power density decreases and is greater than 10 dB down from the plotted wave under small signal conditions.

#### 9. Environmental Characteristics

##### a. Temperature

The specifications require that the tube exhibit less than 0.3 dB variation in power output over the temperature range of  $-20$  to  $+75^{\circ}\text{C}$  measured on the baseplate to which the tube is attached. The WJ-395 S/N 14 exhibited an output power variation of 0.05 dB at a fixed input drive level over the required temperature range.

Environmental type testing of WJ-395 construction and design was done on tube S/N 10. Thermal tests were done with a thermocouple mounted on the collector hotspot to determine the maximum temperature to which the potting material would be subjected. The tube was fastened to an aluminum baseplate and placed into a temperature

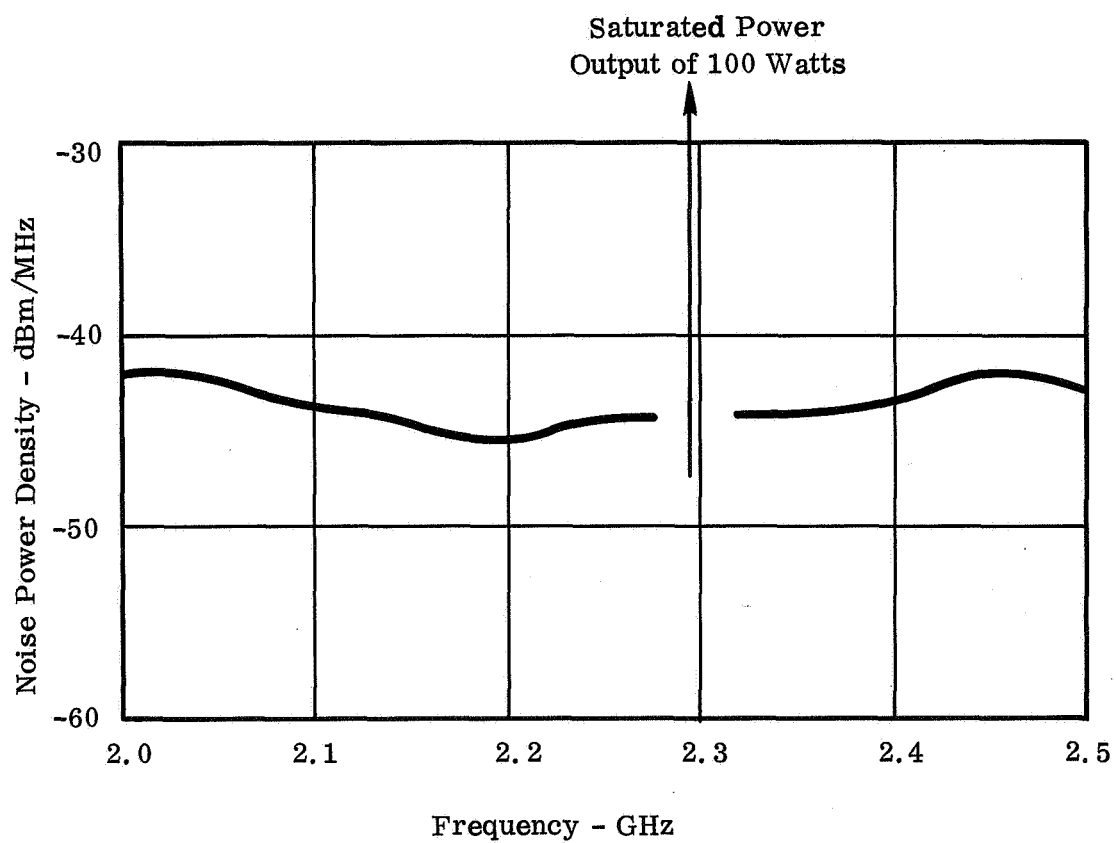


Fig. 15 - Noise power density vs. frequency with a saturated carrier at 2.295 GHz. Helix voltage = 2600 volts. Beam current = 110 mA.

chamber at  $-30^{\circ}\text{C}$ . After a one hour soak, the tube was turned on and temperature and power measurements were made as a function of time as the assembly warmed up. On reaching  $90^{\circ}\text{C}$  baseplate temperature, water cooling of the baseplate was begun and it was stabilized at  $86^{\circ}\text{C}$ . Later the RF drive was removed and the baseplate was held at  $76^{\circ}\text{C}$ . This simulated the worst case operating condition. The temperature and power output changes as a function of temperature are shown in Table II. It is seen that the maximum change in power output of this tube over the entire temperature range under fixed drive conditions was  $-0.1$  dB. The collector hotspot temperature which corresponds to the highest temperature to which the potting material is subjected reaches a maximum of  $152^{\circ}\text{C}$ . This is  $100^{\circ}\text{C}$  below its rating.

b. Vibration

Vibration tests on S/N 10 were conducted as indicated in Table III. The phase and amplitude modulation measurements were made with a Hewlett-Packard 8410 Network Analyzer system. The tube met the specification requirements.

c. Shock Tests

Shock tests were conducted on S/N 10 as shown in Table IV. With the shock and test equipment available, it was known that meaningful phase modulation data could not be taken at Watkins-Johnson. The tests were run to determine if any permanent changes occurred in the tubes due to shock. The tube was operated with only heater voltage during the test. After five shocks in each plane, the tube was operated and tested for changes in performance. None could be detected.

At a later time, operating shock tests were conducted on the tube at JPL. The tube met the specifications for phase modulation during the shock.

TABLE II

## TEMPERATURE TEST OF WJ-395 S/N 10 ENCAPSULATED TUBE

ELAPSED TIME	BASEPLATE TEMP °C	COLL. HOTSPOT TEMP °C	$\Delta T$ °C	RF POWER INPUT dBm	RF POWER OUTPUT dBm	$\Delta P_{OUT}$ dB	$I_H$ mA
1 HR	-30°	-30°	(COLD SOAK, NON-OPERATING)				
0	-18°	---	---	14.3	50.10	0	16.0
6 MIN	1°	---	---	14.3	50.10	0	15.0
18.5 MIN	35°	54°	19°	14.3	50.10	0	13.0
38.0 MIN	69.5°	97°	27.5°	14.3	50.05	-.05	12.0
48.0 MIN	80°	108°	28°	14.3	50.05	-.05	12.2
56 MIN	90	---	---	14.3	50.00	-.10	12.5
<u>WATER COOLING ON</u>							
68 MIN	86°	116°	30°	14.3	50.00	-.10	12.5
<u>RF TURNED OFF</u>							
1 HR 20 MIN	76°	152°	76°	0	0	---	1.1

OPERATING CONDITIONS:

$V_H = 2575$  V      FREQ. = 2.25 GHz  
 $I_o = 120$  mA  
 $V_{COLL} = 2150$  V



TABLE III

VIBRATION TESTS OF WJ-395 S/N 10 ENCAPSULATED TUBE

A. NOISE,  $0.2 \text{ g}^2/\text{cps}$  FROM 300 TO 1000 cps WITH A 6 dB PER OCTAVE ROLL-OFF FROM 1000 TO 2000 cps, A 3 dB PER OCTAVE ROLL-OFF FROM 300 cps TO 20 cps, AND A 24 dB PER OCTAVE ROLL-OFF BELOW 30 AND ABOVE 2000 cps.

TESTED: 3 MINUTES IN EACH OF 3 PRINCIPAL PLANES.

RESULTS: SPURIOUS PM  $< 0.8^\circ$   
SPURIOUS AM  $< 0.1 \text{ dB}$

THESE VALUES ARE  
NOISE LEVEL OF  
MEASURING SYSTEM

B. WHITE GAUSSIAN NOISE, 5.0 g rms, BAND LIMITED BETWEEN 15 AND 2000 cps PLUS A 2.0 g rms SINUSOID SUPERIMPOSED ON THE NOISE BETWEEN 15 AND 40 cps.

C. WHITE GAUSSIAN NOISE, 5.0 g rms, BAND LIMITED BETWEEN 15 AND 2000 cps PLUS A 9.0 g rms SINUSOID SUPERIMPOSED ON THE NOISE BETWEEN 40 AND 2000 cps.

TESTED: SINUSOID SWEEPED FROM 15 TO 2000 cps AND BACK TO 15 cps IN A TOTAL TIME OF 10 MINUTES AT A RATE INCREASING DIRECTLY WITH FREQUENCY IN EACH OF 3 PRINCIPAL PLANES.

RESULTS: SPURIOUS PM  $< 0.8^\circ$   
SPURIOUS AM  $< 0.1 \text{ dB}$

TABLE IV

SHOCK AND ACCELERATION TESTS OF WJ-395 S/N 10

SHOCK

A. 5 200 g,  $0.7 \pm 0.2$  MILLISECOND RISE TIME TERMINAL PEAK SAWTOOTH SHOCKS IN EACH OF 3 ORTHOGONAL DIRECTIONS.

TESTED: 5 200 g, 2.5 MILLISECOND ( $\frac{1}{2}$  AMPLITUDE) DURATION, HALF SINE-WAVE SHOCKS IN X, Y, AND Z DIRECTIONS. THE TEST EQUIPMENT WAS UNABLE TO REALIZE THE SPEC. WAVEFORMS.

OPERATING TESTS COULD NOT BE PERFORMED DURING SHOCK. HEATER WAS OPERATED AND TUBE TESTED AFTER EACH GROUP OF 5 SHOCKS.

RESULTS: NO OBSERVABLE CHANGE IN GAIN OR POWER OUTPUT.

STATIC ACCELERATION

A. ACCELERATION OF  $\pm 14$  g's IN THREE ORTHOGONAL DIRECTIONS FOR 5 MINUTES EACH.

TESTED: 13.9 g FOR 5 MINUTES IN X, Y, AND Z DIRECTION. OPERATING TESTS COULD NOT BE PERFORMED DURING ACCELERATION. HEATER VOLTAGE WAS APPLIED.

RESULTS: NO OBSERVABLE CHANGE IN GAIN OR POWER OUTPUT.

d. Acceleration Tests

Acceleration tests were conducted on S/N 10 as shown in Table IV. The centrifuge used in the acceleration tests had no high voltage slip-rings and as a result, only heater voltage could be applied during the tests. The tube was tested for a change in performance after acceleration in three planes.

The tests showed no observable change in gain, power output or current distribution to the tube elements as a result of the environment to which the tubes were subjected.

e. Vacuum

A number of different thermal-vacuum tests have been performed on tubes. It has been determined that the heat transfer system for conducting the heat from the tube body and the collector to the bottom of the capsule performs satisfactorily under thermal-vacuum conditions and causes the tube to be adequately cooled.

High vacuum tests have shown some difficulty with voltage breakdown in the potting insulation. The problem has been traced to air bubble inclusions in the potting material. This problem has been corrected by constructing a special double vacuum potting system which eliminates the possibility of air bubble inclusions during the potting process.

The deliverable tube has been potted with this technique, but the final performance results await tests in JPL's high vacuum chamber.

Theoretical calculations indicate that there is a possibility that multipactor breakdown could occur in the RF connectors of the tube under space vacuum conditions at the 100 watt level. To combat this possibility, the OSM connectors on the tube have been modified to provide for interlocking dielectric parts. The female connectors on the tube have been changed so that they will accept either a standard OSM connector or a connector with modified dielectric. In this way normal testing can be accomplished with standard connectors while a special mating connector will be required only under critical test or use conditions.

### C. Physical Description

A photograph of the tube is shown in Fig. 16. It is of metal-ceramic construction. The conduction cooled collector assembly is seen at the left, the body with magnets in place for preliminary testing at center and the electron gun is at the right.

A photograph of the encapsulated tube is shown in Fig. 17. It is enclosed in an aluminum capsule. Insulation is obtained with vacuum potted silicone rubber.

The tube weighs 2.35 pounds. An outline drawing is shown in Fig. 18.

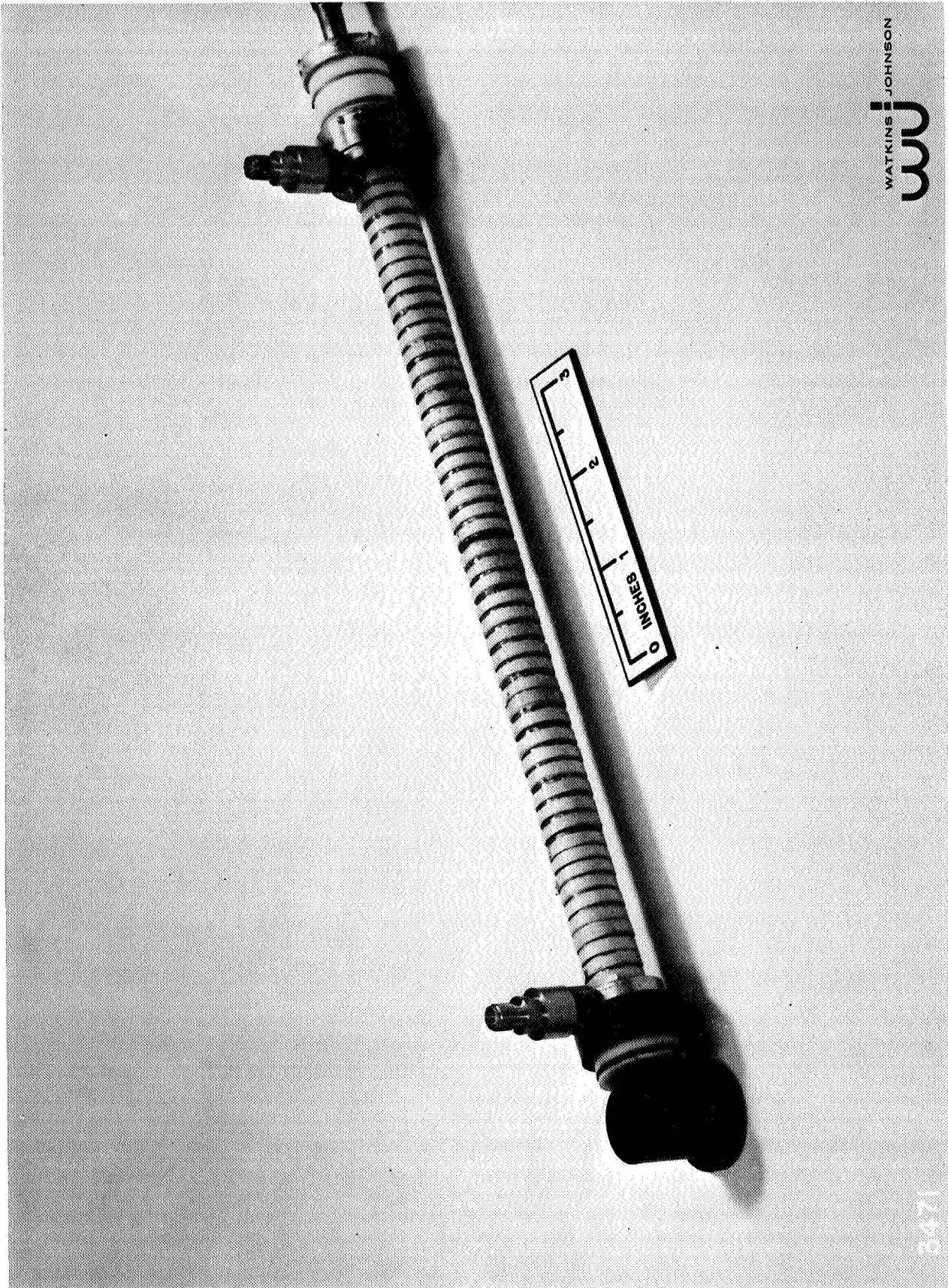


Fig. 16 - Photograph of a WJ-395 tube which is prepared for preliminary test. Collector electrode is at left, focusing magnets are at center and the electron gun is at the right.



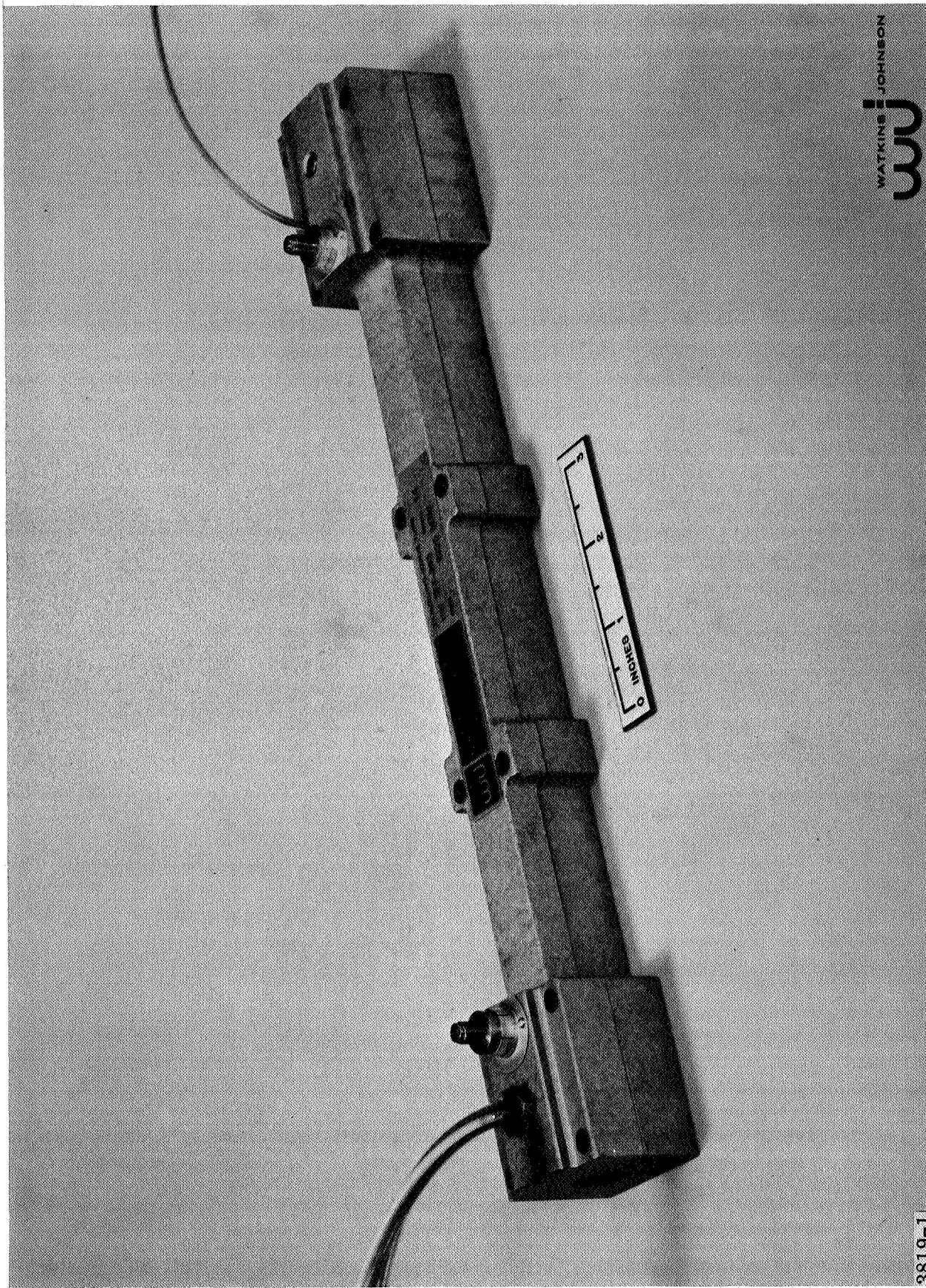
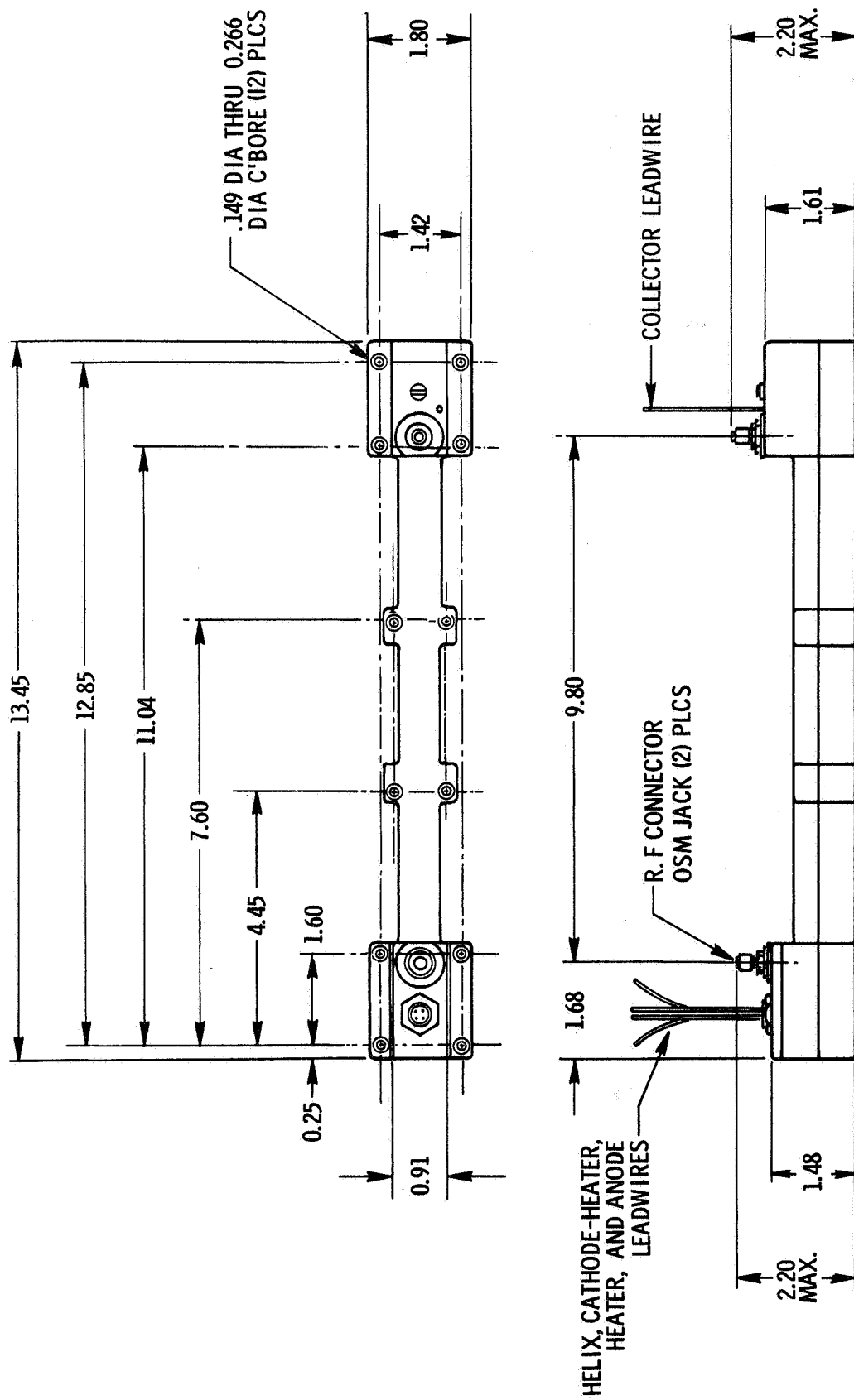


Fig. 17 - Photograph of WJ- 395 S/N 14 after encapsulation. All cooling takes place by conduction through the bottom surface.



## REFERENCES

1. Roberts, L. A., "The Design and Performance of a High Efficiency Traveling-Wave Tube, The WJ-274", Final Report, Phase I, Contract No. NAS1-3766, Watkins-Johnson Company, May 1966.
2. Niclas, K. B. and Gerchberg, R. W., "New Concepts for Achieving High Efficiency in Traveling-Wave Tubes", Quarterly Reports No. 2 and 3, Contract No. DA28-043 AMC-00076 (E), Watkins-Johnson Company, August 1964 through January 1965.
3. Niclas, K. B. and Gerchberg, R. W., "New Concepts for Achieving High Efficiency in Traveling-Wave Tubes", Quarterly Report No. 4, February 1965 through April 1965.
4. Niclas, K. B. and Gerchberg, R. W., "New Concepts for Achieving High Efficiency in Traveling-Wave Tubes", Quarterly Reports No. 5 and 6, May 1965 through October 1965.
5. Roberts, op. cit., pp. 19 - 26.
6. Gerchberg, R. W., Niclas, K. B., and Frost, R. D., "New Methods Leading to High Efficiency in Traveling-Wave Tubes", Final Report, Contract No. DA28-043 AMC-02004 (E), September 1967.
7. Scott, Allan W., "Why a Circuit Sever Affects Traveling-Wave Tube Efficiency", IRE Trans. on Electron Devices, vol. ED-9, No. 1, January 1962, pp. 35 - 40.
8. Pierce, J. R., Traveling-Wave Tubes, D. Van Nostrand Co., 1950.